

Chemosphere

Elsevier Editorial System(tm) for

Manuscript Draft

Manuscript Number: CHEM62554R1

Title: Zero valent iron and goethite nanoparticles as new promising remediation techniques for As-polluted soils

Article Type: Research paper

Section/Category: Treatment and Remediation

Keywords: Arsenic; soil pollution; nZVI; goethite nanoparticles; immobilization; brownfield

Corresponding Author: Dr. Jose Luis R. Gallego, Ph.D.

Corresponding Author's Institution: University of Oviedo

First Author: Diego Baragaño

Order of Authors: Diego Baragaño; Juan Alonso; Jose Luis R. Gallego, Ph.D.; Carmen Lobo, Ph.D.; Mar Gil-Díaz, Ph.D.

Abstract: The capacity of two iron-based nanomaterials, namely goethite nanospheres (nGoethite) and zero valent iron nanoparticles (nZVI), to immobilize As in a polluted soil was evaluated and compared. The composition and morphology of the products were studied by energy dispersive X-ray analysis and transmission electron microscopy, while zeta potential and average sizes were determined by dynamic light scattering. To assess As immobilization, soil subsamples were treated with nGoethite or nZVI at a range of Fe doses (0.5%, 2%, 5% and 10%) and then studied by the TCLP test and the Tessier sequential extraction procedure. The influence of both nanoparticles on As speciation was determined, as was impact on soil pH, electrical conductivity, Fe availability and phytotoxicity (watercress germination). For nZVI, notable results were achieved at a dose of 2% (89.5% decrease in As, TCLP test), and no negative effects on soil parameters were detected. Indeed, even soil phytotoxicity was reduced and only at the highest dose was a slight increase in As³⁺ detected. In contrast, excellent results were obtained for nGoethite at the lowest dose (0.2%) (82.5% decrease in As, TCLP test); however, soil phytotoxicity was increased at higher doses, probably due to a marked enhancement of electrical conductivity. For both types of nanoparticle, slight increases in Fe availability were observed. Thus, our results show that both nZVI and nGoethite have the capacity to effectively immobilize As in this brownfield. The use of lower doses of nGoethite emerges as a promising soil remediation strategy for soils affected by As pollution.

Dear Editor,

We have the pleasure to attach a revised copy of the manuscript " Zero valent iron and goethite nanoparticles as new promising remediation techniques for As-polluted soils" by Diego Baragaño, Juan Alonso, José Luis R. Gallego, M. Carmen Lobo and Mar Gil-Díaz.

Thank you very much for your positive comments and for sending the constructive suggestions made by reviewers. We have read carefully all comments and modified the submission accordingly. Please find below a detailed list of changes.

Reviewer #2: This paper describes two iron-based nanomaterials immobilize As in a polluted soil. The objectives of the paper are interesting; the work is nice and important. The manuscript is nicely written. So, I suggest a major revision before the acceptance of this paper.

1. The highlight 2 "Only high doses of nGoethite caused phytotoxicity", what do high doses of nGoethite mean? Please clarify.

Highlight 2 has been modified in order to clarify the doses than generated phytotoxicity.

2. The pH of soil is high in this study, please forecast the effect of material on low pH soil, example pH 4-5.5.

This was discussed (for nZVI) in Gil-Díaz et al 2017. Viability of a nanoremediation process in single or multi-metal(loid) contaminated soils. J. Hazard. Mater. 321, 812–819.

In our case, although a detailed experimentation should be carried out to answer this question, it seems reliable that nZVI addition would slightly increase soil pH if this is initially acidic, and therefore may provoke As immobilization thereby improving phytotoxicity. On the contrary, giving the acidic pH of the commercial nGoethite used, these nanoparticles should not affect a hypothetical initial acidic soil pH value and should not generate significant changes. At any case, in our current study it was demonstrated that high doses were not needed to obtain notable stabilization effects, and as a consequence moderate doses in real-scale treatments would not promote notable changes in soil pH. Overall, the study of these nanomaterials on low pH soil should be of course interesting (for instant in conditions of acid mine drainage or with acidic soils), thus it will be evaluated in forthcoming works.

3. What is the final morphology of iron after iron-based nanomaterials added soil.

After zero valent iron nanoparticles addition to the soil, it can be expected, as reported in many studies, that nanoparticles suffer oxidation, a subsequent increase in their size and aggregation, as it has been proved for instance in a previous work through SEM images (Gil-Díaz et al, 2019). On the other hand, goethite nanoparticles are iron oxy-hydroxides, so they would be generating iron oxide aggregates in soils also.

4. Please confirm the mechanism of iron-based nanomaterials on the pH and EC of soil.

The effect of nZVI on pH and EC values of soil has been described in lines 303-304 of the revised manuscript: "The application of nZVI did not affect pH or EC at any of the doses tested".

Respect to nGoethite, the decrease on the soil pH is due to the acidic pH of the suspension used. In case of EC, As immobilization has been almost completed at moderate doses, so we suggest that the EC increase in the highest doses (D4) is probably caused by an excess of

nanoparticles which have not interacted with As. This hypothesis has been included in the revised manuscript in lines 309-311.

5. What is the reason why NZVI significantly reduces phytotoxicity at all experimental doses?

The phytotoxicity becomes better as the As immobilization is improved as the doses are increased; i.e. as higher quantities of As are not bioavailable as soil phytotoxicity is decreased.

Reviewer #3: This paper reports a comparison study using nZVI versus goethite nanoparticles (nGoethite) in the remediation of arsenic (As) contaminated soils. Various aspects including the As leaching, As speciation, and phytotoxicity of nZVI versus nGoethite treated soils are evaluated and compared. The study is generally interesting and could be useful to inform remediation strategies in As contaminated soils using iron-based nanotechnology. I recommend publication of this work after consideration of the points outlined as follows.

1. Batch experiments: the NP doses used is based on the same percentage of Fe. This means the actual doses for nGoethite would be higher than nZVI at the same Fe weight %. If the comparison is based on the actual weight % added to the soil rather than just Fe, how would that affect the results of the study. Please discuss.

This is a very interesting question. Using the same quantity of iron per gram of soil in both treatments allowed comparisons of the phytotoxicity data and especially of Fe availability, both important parameters in order to analyse potential toxicity and nanoparticles effects. However, this decision as the referee indicates might condition As immobilization, given that goethite nanoparticles are smaller than nZVI, as demonstrated in the characterization section (Figure S2), thus their potential capabilities to adsorb As are higher (higher surface area), as it has been remarked in lines 204-210.

2. The method section, especially section 2.4, in its current form is a bit ambiguous and not easy to follow. For example, line 130-137 indicates that 20-g subsamples of soil was treated with each type of NPs with varied doses in 50-mL plastic vials. Then Line 138-141 indicates that DI water (at what volume?) was added to the soil samples. It is followed by the description of As leaching procedures in Line 142-150. It is confusing if the adding DI water is part of the leaching procedures (e.g., TCLP or Tessier sequential extraction). Was adding DI water to the NPs treated soil samples meant to measure pH and EC changes only? This question is asked because line 149-150 which belongs to the As leaching procedure paragraph also indicates that EC and pH were measured. This whole section needs clarification or probably re-organization.

The DI water was used to facilitate an intimate blend between the soil particles and the nanoparticles suspension. The total amount of "liquid" used (DI water + water in the NPs suspension) was selected in accordance to the water holding capacity of the soil and to the doses of nanoparticles suspension used in each trial. This methodology was followed also in previous works (see Gil-Díaz et al., 2017, references therein, and previous studies of the same group).

Samples were air dried after batch experiments and thus As leaching was determined on dry samples, and pH was measured in a new resuspension of soil in distilled water (1:2.5). In order to clarify the procedure, this information was added in lines 139, 142 and 152.

3. Line 151-155 describes As speciation measurements, but the procedure is not clear. For example, in line 151: 0.1 g of soil (NPs treated?) and an extracting agent (1 M H₃PO₄ + 0.1 M ascorbic acid) were placed in a microwave vessel and digested. What volume of the extracting agent was used here? What is the microwave heating program used? In the analysis of As speciation, the column specification and mobile phase flow rates should be described.

The methodology used for As speciation has been detailed in the revised manuscript (lines 153-159). The analysis has been carried out using 0.1 g of soil (treated and un-treated), although in case of treated soils, a calculation to eliminate the dilution effect generated by the presence of nanoparticles was done.

4. This study has many extraction and digestion methods (e.g., line 104-109, 151-153). It is encouraged to include the mass recovery of these methods.

A near-total extraction of As is very difficult to be done and should require peroxide total fusion methods (not available in our labs) given that an approach using HF would promote As erratical volatilization. Therefore we selected a "pseudototal" extraction using aqua regia digestion. As regards a comparison between this pseudototal digestion and the digestion used for speciation analyses, we determined a difference of approximately 25% lower yields for the second one. This was expectable given that the second extraction is softer than the aqua regia one. However, the purpose of As speciation assessment was to observe differences between un-treated and treated samples, thus the results (Table 1) shows the relation of As(III) and As(V) in percentage based on the sum of both species and not in the pseudo-total concentration determined by aqua regia digestion. This was indicated in the revised manuscript (see Table 1 legend).

5. nGoethite is a commercial product from Sigma Aldrich. Please add the catalog # of this product.

The catalog data were added in line 114.

6. nZVI and nGoethite appear strongly aggregated (Figure1 A&B) in the TEM images presented. I don't see that these NPs distribute uniformly as claimed (line 202). This can be anticipated in the TEM sample preparation where NPs could aggregate during the drying step. Perhaps DLS size distribution in the aqueous solution can be used to help evaluate the sizes and aggregation of NPs used. It is therefore suggested to add this information.

We agree with this comment of the reviewer. Accordingly, the size of nanoparticles distribution has been included in the supplementary material by means of two graphics. In addition, the description of the sizes of the nanoparticles was modified in lines 204-210 and it is now based on DLS results (Figure S2 was added) while the comments about TEM images were partially eliminated.

7. The solution chemistry (pH, ionic strength, ect.) affects the zeta potential of NPs. What solution chemistry was used in the measurement of zeta potentials reported in line 208 and 211? The zeta potential was used to infer the sorption of As onto nGoethite and nZVI in the leaching studies. What would be the zeta potentials of NPs in the leaching solutions? Are the solution chemistry the same as that used to measure zeta potentials in line 208 and 211?

Zeta potential of nanoparticles was measured in order to characterize the nanoparticles surface, so the measures were carried out on the nanoparticles suspension (results reported in lines 213-217). However, the question raised by the reviewer is very interesting. Once

nanoparticles are in the soil, the interaction between nanoparticles and As can be very quick due to their high reactivity. Therefore, once nanoparticles interact with soil matrix and pollutants (and with other nanoparticles) they form aggregates and then the surface area and zeta potential are modified. In this work, this idea has not been developed given that we were interested in the initial zeta potential to be able to adsorb As (as it happened). Nevertheless; the measurement of zeta potentials after mixing with soil would be interesting for forthcoming works in order to study the stability and morphology of nanoparticles in soil after nanoremediation or even to recover those using magnetic fields or other approaches. We really thank to the reviewer for this idea.

8. It is interesting that the EC was increased with added nGoethite (table 2). What would lead to the increased EC with increased nGoethite dose added in contrast to nZVI? Please discuss. The EC unit in Table 2 should be added.

In case of nGoethite, As immobilization has been almost completed at moderate doses, so we suggest that the EC increase (doses D3 and specially D4) is probably caused by an excess of nanoparticles which have not reacted with As, which was already immobilized. This hypothesis has been included in the manuscript in lines 309-311. EC units were added in table 2.

9. It would be useful to mention the purpose of the 3.3.4 Fe availability study. Does it impact soil ecosystem and how?

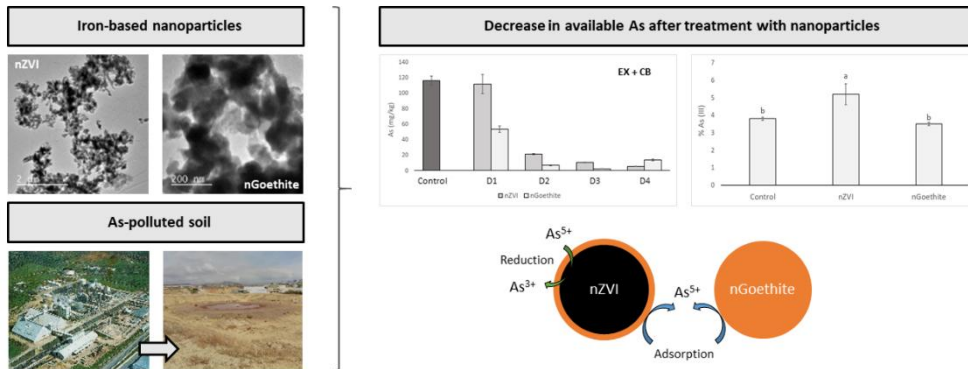
Fe availability study was carried out in order to evaluate the potential impact of nZVI and nGoethite in soil ecosystem. As mentioned in the introduction (line 65-69), risks due to the potential toxicity of iron nanoparticles have been profusely discussed in other works by evaluating Fe availability and effects on phytotoxicity (Cagigal et al., 2018 and references therein; Gil-Diaz and Lobo, 2018). In addition, an increase on Fe availability may generate negative effects on plants. Thus, one of the objectives of this study is to determine the effects of the two types of nanoparticles used on Fe availability and soil phytotoxicity. In order to clarify the motivation of this objective, it was modified the text in line 84.

10. Although citation is given, it would be useful to also briefly describe how soil extracts were obtained in the phytotoxicity study.

Description of how soil extracts were obtained was added in methodology (lines 161-163).

Zero valent iron and goethite nanoparticles as new promising remediation techniques for As-polluted soils (Baragaño et al., 2019)

Graphical abstract



Zero valent iron and goethite nanoparticles as new promising remediation techniques for As-polluted soils

D. Baragaño^a, J. Alonso^b, J.R. Gallego^a, M.C. Lobo^b, M. Gil-Díaz^b

^a INDUROT, Environmental Technology, Biotechnology, and Geochemistry Group, Universidad de Oviedo, Campus de Mieres, 33600 Mieres, Asturias, Spain

^b IMIDRA, Instituto Madrileño de Investigación y Desarrollo Rural, Agrario y Alimentación, Finca "El Encín", Alcalá de Henares, 28800, Madrid, Spain

Abstract

The capacity of two iron-based nanomaterials, namely goethite nanospheres (nGoethite) and zero valent iron nanoparticles (nZVI), to immobilize As in a polluted soil was evaluated and compared. The composition and morphology of the products were studied by energy dispersive X-ray analysis and transmission electron microscopy, while zeta potential and average sizes were determined by dynamic light scattering. To assess As immobilization, soil subsamples were treated with nGoethite or nZVI at a range of Fe doses (0.5%, 2%, 5% and 10%) and then studied by the TCLP test and the Tessier sequential extraction procedure. The influence of both nanoparticles on As speciation was determined, as was impact on soil pH, electrical conductivity, Fe availability and phytotoxicity (watercress germination). For nZVI, notable results were achieved at a dose of 2% (89.5% decrease in As, TCLP test), and no negative effects on soil parameters were detected. Indeed, even soil phytotoxicity was reduced and only at the highest dose was a slight increase in As³⁺ detected. In contrast, excellent results were obtained for nGoethite at the lowest dose (0.2%) (82.5% decrease in As, TCLP test); however, soil phytotoxicity was increased at higher doses, probably due to a marked enhancement of electrical conductivity. For both types of nanoparticle, slight increases in Fe availability were observed. Thus, our results show that both nZVI and nGoethite have the capacity to effectively immobilize As in this brownfield. The use of lower doses of nGoethite emerges as a promising soil remediation strategy for soils affected by As pollution.

Keywords

Arsenic; soil pollution; nZVI; goethite nanoparticles; immobilization; brownfield

Zero valent iron and goethite nanoparticles as new promising remediation techniques for As-polluted soils (Baragaño et al., 2019)

Highlights

nZVI and nGoethite immobilized As efficiently in a polluted soil.

Doses higher than 1% of nGoethite caused phytotoxicity.

Nanoparticle addition did not lead to a considerable increase in Fe availability.

nGoethite emerges as an interesting alternative to nZVI for As immobilization.

1 **Zero valent iron and goethite nanoparticles as new promising** 2 **remediation techniques for As-polluted soils**

3 D. Baragaño^a, J. Alonso^b, J.R. Gallego^a, M.C. Lobo^b, M. Gil-Díaz^b

4 ^a INDUROT, Environmental Technology, Biotechnology, and Geochemistry Group, Universidad
5 de Oviedo, Campus de Mieres, 33600 Mieres, Asturias, Spain

6 ^b IMIDRA, Instituto Madrileño de Investigación y Desarrollo Rural, Agrario y Alimentación, Finca
7 “El Encín”, Alcalá de Henares, 28800, Madrid, Spain

8 **Abstract**

9 The capacity of two iron-based nanomaterials, namely goethite nanospheres (nGoethite) and
10 zero valent iron nanoparticles (nZVI), to immobilize As in a polluted soil was evaluated and
11 compared. The composition and morphology of the products were studied by energy
12 dispersive X-ray analysis and transmission electron microscopy, while zeta potential and
13 average sizes were determined by dynamic light scattering. To assess As immobilization, soil
14 subsamples were treated with nGoethite or nZVI at a range of Fe doses (0.5%, 2%, 5% and
15 10%) and then studied by the TCLP test and the Tessier sequential extraction procedure. The
16 influence of both nanoparticles on As speciation was determined, as was impact on soil pH,
17 electrical conductivity, Fe availability and phytotoxicity (watercress germination). For nZVI,
18 notable results were achieved at a dose of 2% (89.5% decrease in As, TCLP test), and no
19 negative effects on soil parameters were detected. Indeed, even soil phytotoxicity was
20 reduced and only at the highest dose was a slight increase in As³⁺ detected. In contrast,
21 excellent results were obtained for nGoethite at the lowest dose (0.2%) (82.5% decrease in As,
22 TCLP test); however, soil phytotoxicity was increased at higher doses, probably due to a
23 marked enhancement of electrical conductivity. For both types of nanoparticle, slight increases
24 in Fe availability were observed. Thus, our results show that both nZVI and nGoethite have the
25 capacity to effectively immobilize As in this brownfield. The use of lower doses of nGoethite
26 emerges as a promising soil remediation strategy for soils affected by As pollution.

27 **Keywords**

28 Arsenic; soil pollution; nZVI; goethite nanoparticles; immobilization; brownfield

29 **1. Introduction**

30 The closure of industrial and mining facilities has brought to light the presence of large
31 volumes of contaminated soil worldwide (Adriano, 2001; Gallego et al., 2016; Santucci et al.,
32 2018). These sites, known as brownfields (Marker, 2018), are particularly common in areas
33 with a history of heavy industrial activity. Among the pollutants found in brownfield soils,
34 Potentially Toxic Elements (PTEs), such as Pb, As, Cu or Zn, are some of the most frequent due
35 to their release during industrial processes (Lado et al., 2008; Magiera et al., 2018),
36 atmospheric deposition (Boente et al., 2017; Davis and Birch, 2011) and inappropriate
37 dumping of waste (Alekseenko et al., 2018; Rao, 2014). PTEs, even at low concentrations, can
38 pose a serious threat to human health and ecosystems (Fraga et al., 2005; Gopalakrishnan et
39 al., 2015; Irem et al., 2019).

40 In particular, arsenic (As) is a highly toxic and carcinogenic element and as such it compromises
41 ecosystem quality and human health (Hopkins et al., 2009). In general, As(V) and As(III) are the
42 most common stable oxidation states of this heavy metal in soils (Aide et al., 2016),
43 As(III) being more toxic than As(V). Classical methods for the remediation of As-contaminated
44 soils require physical/chemical methods such as solidification/stabilization, soil washing, and
45 electrokinetics, or biological strategies such as phytoremediation (Forján et al., 2016; Gonzalez
46 et al., 2019; Hasegawa et al., 2015; Khalid et al., 2017; Kumpiene et al., 2008; Mesa et al., 2017;
47 Pérez-Sanz et al., 2013). Among the most common techniques used in situ, those based on
48 arsenate immobilization through adsorption and surface complexation on iron-based
49 compounds have been widely studied (Hartley et al., 2004; Hartley and Lepp, 2008; Chen and
50 Li, 2010; Komárek et al., 2013). Sorption on iron oxides was found to lead to inner-sphere
51 surface complexation, including monodentate, bidentate mononuclear, and bidentate
52 binuclear complexes (Fendorf et al., 1997; Gao et al., 2006; Hua et al., 2012; Rahimi et al.,
53 2015).

54 Recent years have witnessed the development of nanoremediation as a novel technique to
55 immobilize heavy metal(oid)s, especially methods involving the addition of nanoscale zero
56 valent iron nanoparticles (nZVI) to stabilize and reduce PTE availability (Gil-Diaz et al., 2017a,
57 2017b, 2019; Gonçalves, 2016; Mueller et al., 2012; O'Carroll et al., 2013). nZVI usually present
58 acicular shapes, thus increasing the specific surface of granular iron and achieving higher
59 reactivity due to their size (O'Carroll et al., 2013). Several studies have shown that nZVI
60 effectively immobilize As in water samples and soils (Gil-Díaz et al., 2017a; Kim et al., 2012;
61 Rahmani et al., 2010), even in field conditions (Gil-Díaz et al., 2019). In aqueous solutions, nZVI
62 react with water and oxygen to form an outer Fe (hydr)oxide layer, so these particles present
63 a core-shell structure (O'Carroll et al., 2013). In this context, differences in the structural
64 properties of nZVI strongly influence the reactivity and aging of the particles (Fajardo et al.,
65 2015; Gil-Díaz et al., 2017b, 2016a). In addition, risks due to the potential toxicity of nZVI have
66 been reported and should be taken into account (Cagigal et al., 2018; Gil-Diaz and Lobo, 2018).
67 In this regard, nanoparticle (NP) dose, exposure time, oxidation rate and Fe availability are
68 parameters to be considered (Fajardo et al., 2012; Gil-Diaz et al., 2017b; Li et al., 2010; Saccà
69 et al., 2014).

70 To overcome these difficulties, other NPs based on Fe oxides have been used for
71 environmental remediation purposes. In this regard, they have shown greater stability than
72 nZVI when used for PTE removal from water (Chen and Li, 2010; Rahimi et al., 2015) or even
73 from soils (Waychunas et al., 2005; Zhang et al., 2010). In particular, iron oxy-hydroxide (α -
74 FeOOH) is a natural oxide mineral, known as goethite, which promotes contaminant
75 sequestration (including As) by sorption processes (Giménez et al., 2007; Waychunas et al.,
76 2005). Indeed, even synthetic goethite has been produced (Atkinson et al., 1968) and applied
77 for As immobilization (O'Reilly et al., 2010). In this context, synthesized goethite have recently
78 been used successfully to remove Cu and Pb from polluted water, achieving better results than
79 other iron oxides (Chen and Li, 2010; Rahimi et al., 2015). However, to the best of our

80 knowledge, despite the great potential of goethite as an adsorbent, the capacity of goethite
81 NPS (nGoethite) to remove As from water or immobilize As in soils has not been tested.

82 The main objectives of this work are: i) to compare the effectiveness of commercial nZVI and
83 nGoethite to immobilize As in an industrial polluted soil; and ii) **to determine potential toxic**
84 **effects of these nanoparticles by means of Fe availability and soil phytotoxicity evaluation.**

85 **2. Materials and methods**

86 **2.1 Samples**

87 Samples were taken from polluted soils in one of the main former fertilizer plants in southern
88 Spain (Andalusia), which operated for almost forty years until its closure in 1997. Following its
89 dismantling in 2001, characterization studies revealed areas with concentrations of As
90 exceeding soil screening levels (Baragaño et al., 2018).

91 Within the area affected by As pollution, a 5-kg composite soil sample was collected from the
92 surface layer (0 – 25 cm) with a manual auger. It was then air-dried, homogenized and sieved
93 (<2 mm) prior to analysis.

94 **2.2 Analyses**

95 The physico-chemical properties of the soil were determined in representative subsamples
96 using the Spanish official methodology (MAPA, 1994). In brief, organic matter was determined
97 using the Walkley-Black method (dichromate oxidation); pH and electrical conductivity (EC)
98 were measured in a 1:2.5 soil-to-water ratio; total nitrogen content was quantified by the
99 Kjeldahl method; the percentage of carbonates was measured using a Bernard calcimeter; and
100 available nutrients (Ca, K, Mg, Na) were extracted with 0.1 N ammonium acetate and
101 quantified using a flame atomic absorption spectrometer (AA240FS, Varian). Grain size was
102 characterized by wet-sieving and laser diffraction spectroscopy using the Aqueous Dry Module
103 of an LS 13 320MW system (Beckman Inc. Coulter).

104 **Pseudo-total** metal(loid) concentrations were determined after acid digestion with a mixture
105 of 6 mL nitric acid (69% purity) and 2 mL of hydrochloric acid (37% purity), in a microwave
106 reaction system (Multiwave Go, Anton Paar GmbH). In the digestion extract, the
107 concentrations of Fe, Cd, Cr, Cu, Ni, Pb and Zn were quantified by flame atomic absorption
108 spectrometry (FAAS) (AA240FS, Varian) and As by graphite furnace atomic absorption
109 spectrometry (GFAAS) with Zeeman Correction (AA240Z, Varian).

110 **2.3 Iron-based nanoparticles characterization**

111 Two types of commercially iron NPs were purchased: Zero valent iron NPs (nZVI) called
112 NANOFER 25S, obtained from Nano Iron s.r.o., (Rajhrad, Czech Republic), and goethite NPs
113 (nGoethite) synthesized by Cerion Advanced Materials (USA) and obtained from Sigma-Aldrich
114 (USA, #796093). The NPs were used immediately after receipt, thereby preventing any
115 chemical alteration, and solutions were covered with aluminium foil to prevent light-induced
116 degradation.

117 Chemical and macro-morphology studies of both types of NP were performed by scanning-
118 electron microscope and energy dispersive X-ray spectroscopy (SEM-EDX) using a JEOL JSM-
119 5600 Scanning Electron Microscope coupled to an Energy Dispersive X-ray analyzer (INCA
120 Energy 200).

121 The size and morphology of the NPs were measured in a JEOL JEM-2100F transmission electron
122 microscope (TEM). For TEM observations, sample preparation involved the dispersion of the
123 NPs in a suspension of water by means of sonication, and deposition on a holey carbon film-
124 coated copper grid and subsequent drying. The mean size of NPs was determined by image
125 analysis and confirmed by dynamic light scattering (DLS) using a Zetasizer Nano ZS (Malvern
126 Panalytical). Finally, to determine surface charge and given that the sorption mechanism
127 between As and iron oxides is a surface phenomenon, the zeta potential of the NPs was
128 determined using a Zetasizer Nano ZS.

129 2.4 Batch experiments and monitoring

130 To test the effectiveness of the NPs for As immobilization, 20-g subsamples of polluted soil
131 were treated with each type of NP at different doses in 50-mL plastic vials. nZVI doses of 0.5%,
132 2%, 5% and 10% (w:w) were selected on the basis of previous studies with other As-polluted
133 soils (Gil-Díaz et al., 2017a, 2017b, 2016a). nGoethite doses of 0.2%, 1%, 2% and 5% were
134 selected in order to facilitate comparison of the effects of the two distinct types of NPs at a
135 similar Fe content per gram of soil, i.e., the amount of Fe added to the soil corresponded to
136 that of the nZVI experiments. Therefore increasing doses of Fe are labeled henceforth as D1,
137 D2, D3 and D4 irrespective of the NPs used.

138 Before beginning the experiments, deionized water was added to the soil samples to achieve
139 water holding capacity **in order to improve nanoparticles and soil contact**. NPs were then
140 applied, except for control tests, which were treated only with deionized water. Experiments
141 were carried out in triplicate. Vials were shaken for 72 h at 100 rpm in a Reax 2 shaker
142 (Heidolph Instrument GmbH & Co. KG). **After shaking, samples were air dried.**

143 To quantify potential As leachability, the TCLP test (Toxicity Characteristic Leaching Procedure)
144 was performed following the USEPA Method 1311 (1992). Furthermore, to determine the
145 potential mobility and availability of As in soil samples, the sequential extraction procedure
146 proposed by Tessier et al. (1979) was also performed. In brief, extracts with reagents of
147 increasing strengths were sequentially added to the subsamples. The following fractions were
148 obtained: exchangeable (EX); bound to carbonates (CB); bound to Fe-Mn oxides (OX); bound to
149 organic matter (OM); and residual (RS). As and Fe concentrations were measured in the
150 extracts following the methodology described in section 2.2. Electrical conductivity (EC) and pH
151 were also measured to evaluate the influence of NP application on soil properties **in a**
152 **suspension of soil and distilled water (1:2.5).**

153 For measuring As species, 0.1 g of soil and 15 mL of the extracting agent (1 M H₃PO₄ + 0.1 M
154 ascorbic acid) were placed in a microwave vessel and digested (Multiwave 3000, Anton Paar
155 GmbH) at 60W for 10 min (Garcia-Manyes et al., 2002). After cooling, the extracts were diluted
156 and filtered (0.45 µm). The As species were separated in a 4.6 mm x 150 mm As Separation
157 Column (Agilent Technologies) fitted to a 1260 Infinity HPLC coupled to a 7700 ICP-MS (Agilent
158 Technologies) using a mobile phase of 2 M PBS (Phosphate Buffered Saline)/0.2 M EDTA (pH =
159 6.0) at a flow of 1 mL/min.

160 **2.5 Soil phytotoxicity**

161 The phytotoxicity of the NP-treated and untreated soil samples was determined using a
162 modified version of the Zucconi test (Zucconi et al., 1985), as described in a previous study (Gil-
163 Díaz et al., 2014). In brief, six watercress (*Nasturtium officinale*) seeds moistened with 6 mL of
164 distilled water (control) or soil extract were placed in triplicate Petri dishes. Soil extracts were
165 obtained by means of 5 g of air-dried in contact with 50 mL of distilled water at 60°C during 30
166 min, followed by filtering with a Whatman paper (541 grade). After two days of incubation in
167 the dark at 26-27°C, the seed germination percentage was calculated and the root length of
168 seedlings was measured. The germination index (GI) was calculated as follows: $GI (\%) = G L_s / L_c$,
169 where G is the percentage of germination obtained with respect to the control values, L_s is the
170 mean root length in the soil extracts, and L_c is the mean root length in the control.

171 **2.6 Statistical analysis**

172 Data were statistically treated using version 24.0 of the SPSS program for Windows. Analysis of
173 variance (ANOVA) and test of homogeneity of variance were carried out. In the case of
174 homogeneity ($p < 0.05$), a post hoc least significant difference (LSD) test was carried out. If
175 there was no homogeneity, Dunnett's T3 test was performed.

176 **3. Results and discussion**

177 **3.1 Soil characterization**

178 The initial soil properties are shown in Table S1 (Supplementary Material). Results revealed
179 typical characteristics of soils in arid areas, i.e. low organic matter and nitrogen content,
180 alkaline pH and a high carbonate content. The texture was sandy loam. The mean
181 concentrations of Cu, Ni, Pb, Zn, Cr, and Cd were below the current Regional Screening Levels
182 for industrial uses (BOJA, 2015). In contrast, the concentration of As was 30 times more than
183 the maximum permitted levels.

184 **3.2 Nanoparticle characterization**

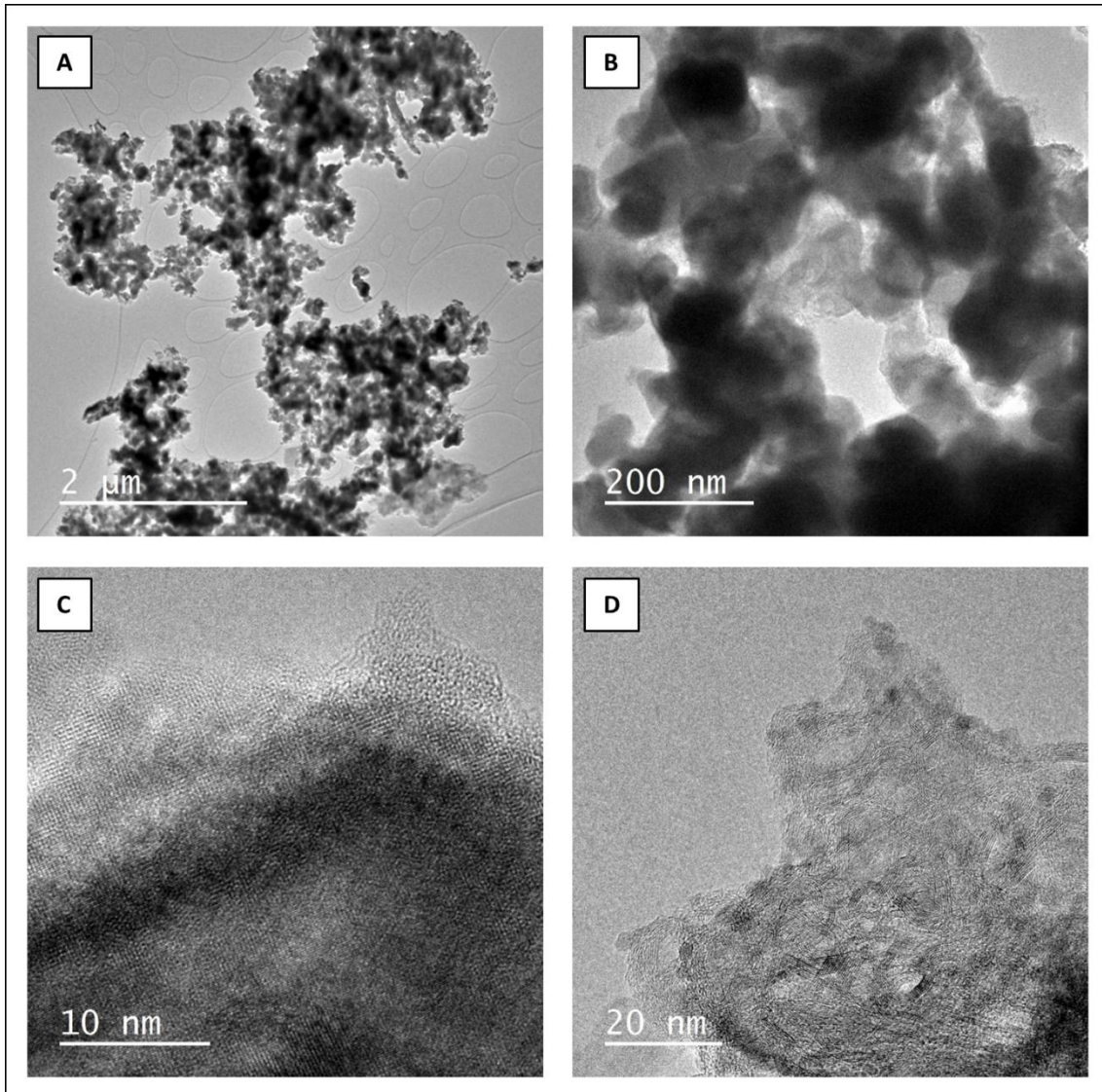
185 In brief, the NANOFER 25S slurry is an aqueous dispersion of stabilized nZVI. According to the
186 commercial specification, its Fe(0) content is 14-18%, and 2-6% of magnetite is also present,
187 the average size of the NPs is around 60 nm, the suspension is strongly alkaline (pH 11-12), and
188 the active surface area is 20 m²/g (additional details are available at www.nanoiron.cz).

189 In contrast, nGoethite are iron oxy-hydroxide (α -FeOOH) NPs dispersed in an aqueous solution.
190 Trace metal analysis revealed low concentrations (total concentration lower than 208 ppm) of
191 Ag, Al, Ba, Cd, Cr, Mg, Pb, Ti, W and Zn and a pH of 3.2 when in suspension, according to the
192 product's certificate of analysis.

193 Although nZVI (NANOFER 25s) have been previously described (Klimkova et al., 2011; Laumann
194 et al., 2013; Schmid et al., 2015), to extend knowledge about nGoethite and compare the two
195 types of NPs, additional analyses were carried out prior to the batch experiments. SEM images
196 of nZVI revealed a surface topography (Figure S1A, Supplementary Material) formed by
197 spheres of regular sizes. However, SEM images of nGoethite (Figure S1B, Supplementary
198 Material) showed a product with a blade shape. Regarding the chemical composition of nZVI
199 (Figure S1C, Supplementary Material) and nGoethite (Figure S1D, Supplementary Material), Fe

200 was found to be the predominant element in the former (more than 80% Fe), and a certain
201 degree of oxidation was observed (less than 20% O). In contrast, iron oxides were the main
202 components of nGoethite (only 60% Fe). Minor components were observed, such as Si and C,
203 which are related to the sample carrier composition.

204 TEM images of nZVI (Figure 1A and 1C) and nGoethite (Figure 1B and 1D) showed that the NPs
205 were not well distributed, probably due to the drying step carried out in the TEM sample
206 preparation. Therefore, DLS analysis was preferred in order to determine the nanoparticles
207 size. Regarding nZVI, the analysis revealed a diameter close to 60 nm which is consistent with
208 the commercial specification, whereas the average diameter of nGoethite was close to 2.7 nm.
209 Comparing size of nanoparticles distribution of both types, nGoethite are one order of
210 magnitude lower and the distribution is narrower than nZVI (Figure S2).



211

212 **Figure 1.** TEM pictures (A and C: nZVI; B and D: nGoethite) of iron nanoparticles.

213 The zeta potential of nZVI was -31.9 mV, a value that is attributed to the polyacrylic acid (PAA)
214 coating used to stabilize the particles, thereby preventing agglomeration caused by counter
215 attractive magnetic and van der Waals forces (Laumann et al., 2013). In contrast, the charge of
216 nGoethite was 86 mV, a positive value consistent with the low pH of the suspension (Giménez
217 et al., 2007).

218

219

220 **3.3 Batch experiment evaluation**

221 *3.3.1 Impact on As availability*

222 The two NP treatments significantly reduced As leachability at the four doses applied, as
223 shown by the TCLP test (Figure 2). Generally, high As immobilization percentages (80-99%)
224 were found in most of the doses, except for D1 of nZVI. However, generally speaking,
225 nGoethite showed greater As immobilization yields (82.5%, 99.3%, 99.7% and 99.8% at
226 increasing doses) than nZVI (41.6%, 89.5%, 96.2% and 97.6%).

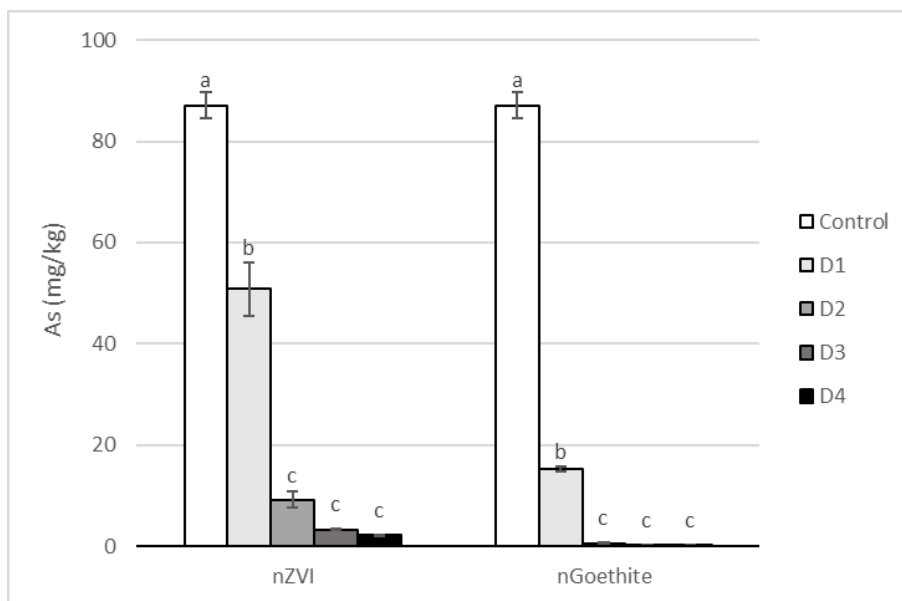


Figure 2. Mean concentration of arsenic (mg/kg) in TCLP extracts. For each type of nanoparticle, bars with the same letter do not differ significantly ($p < 0.05$).

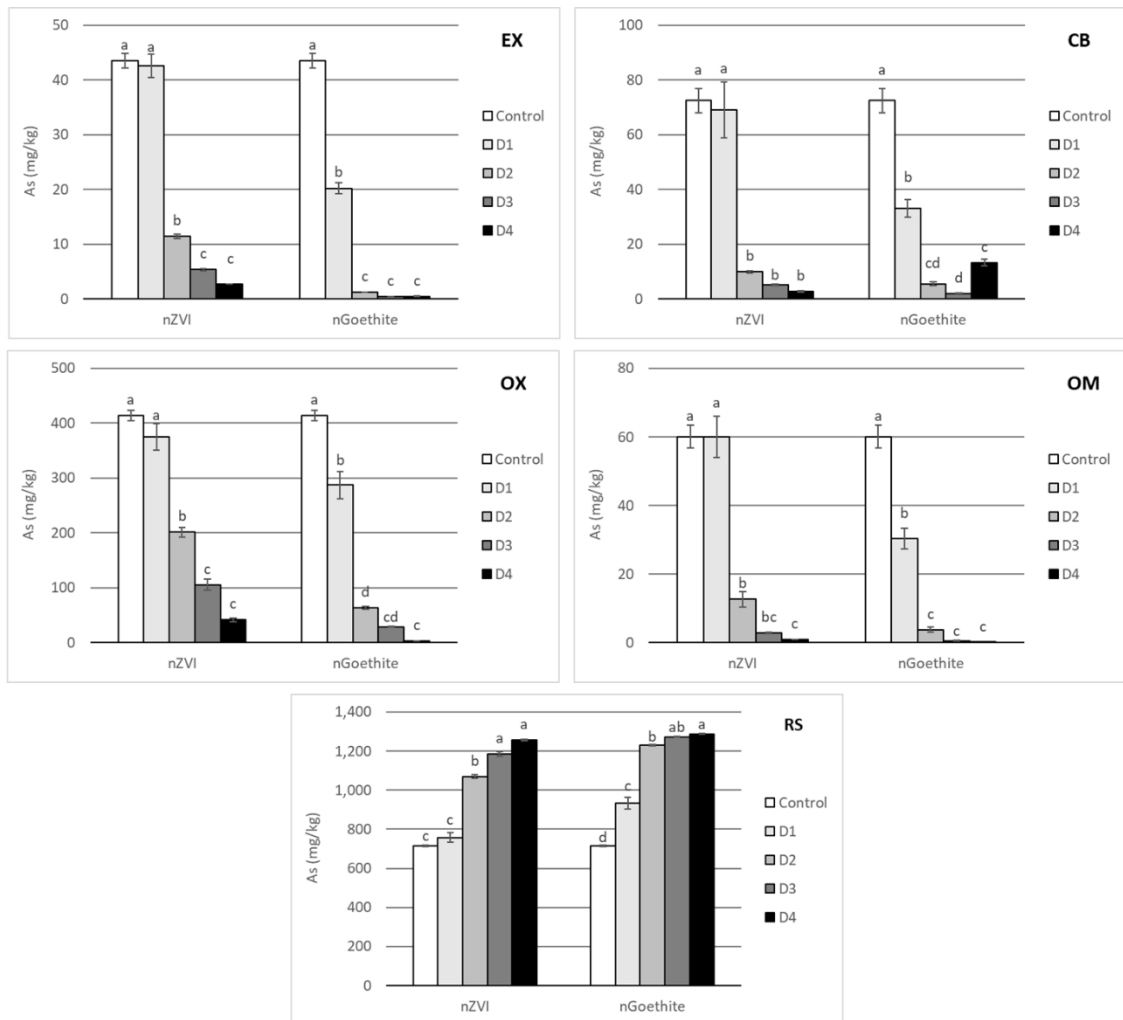
227

228 For all the Tessier fractions (Tessier et al., 1979), a common pattern of As distribution,
229 irrespective of the doses of NPs used, was observed (Figure 3), namely the RS fraction
230 increased, while the other fractions decreased. Only in the case of the lowest dose of nZVI was
231 a significant effect not detected. In this regard, previous studies using nZVI also reported a
232 significant increase in As associated with the RS fraction (Gil-Diaz et al., 2014, 2016, 2017a,
233 2017b).

234 Specifically, the concentration of As in the EX fraction was reduced after the treatment with
235 nZVI at doses D2, D3 and D4 (a reduction ranging from 74% to 94% was observed). In the case
236 of nGoethite, the As concentration in this fraction was reduced at all doses—53% at the lowest
237 dose and up to 99% at the highest. Thus, nGoethite at the lowest dose resulted significantly
238 more efficient than nZVI at reducing the As concentration in the most available fraction. In the
239 CB fraction, As concentration was only significantly reduced at D2, D3 and D4 using nZVI,
240 observing a reduction of between 86% and 96%. In contrast, nGoethite at the lowest dose
241 caused the concentration of As in the CB fraction to fall by 54%, while at higher doses, D2 and
242 D3, it reduced the concentration of this heavy metal in this fraction by up to 92% and 97%
243 respectively. However, at the highest dose, D4, the reduction fell to 82%. This decrease in
244 effectiveness might be due to the agglomeration of the NPs at such a high dosage or by some
245 other effect related to the pH, EC and Fe availability of the soil (Gil-Díaz et al. 2018; Singh and
246 Misra 2015). A similar decrease in As concentration to that observed in the most available
247 fractions was detected in the less mobile OX and OM fractions. Treatment with nZVI, except at
248 the lowest dose tested, led to a reduction in the OX and OM fractions , observing 50-90% and
249 79-99% decreases, respectively. nGoethite at all the doses tested led to significant reductions
250 in the OX and OM fractions, with decreases of 31-99% and 49-99.9% , respectively. Finally, the
251 concentration of As in the RS fraction, the non-available one, was significantly increased after
252 treatment with both types of NP at all doses, especially at the highest dose.

253 The reactivity and effectiveness of NPs for metal(oid) immobilization depend on the properties
254 of the NPs (e.g. size, coating, composition, surface charge) and soil conditions (Gil-Díaz et al.,
255 2017a). Regarding nZVI, this nanomaterial immobilizes As by adsorption onto iron oxides in the
256 shell surrounding the Fe(0) through inner-sphere surface complexation (Gil-Díaz et al., 2017a,
257 2014). Nevertheless, the surface chemistry of goethite differs to that of ZVI and varies with pH.
258 At low pH, the hydroxyl groups at the surface of goethite are doubly protonated ($\equiv\text{FeOH}_2^+$) and
259 the surface charge is thus positive (Giménez et al., 2007; O'Reilly et al., 2010), which is

260 consistent with the positive zeta potential value determined in the nGoethite characterization.
 261 At these acidic pH values, the electrostatic attraction between the negative oxoanions and the
 262 positive charge of the NPs favors adsorption (Siddiqui and Chaudhry, 2018). Therefore, the
 263 lower size of nGoethite NPs compared to nZVI, their corresponding higher specific surface, and
 264 adequate surface charge may explain the greater As immobilization achieved.



265
 266 **Figure 3.** Mean concentration of arsenic (mg/kg) in EX (exchangeable), CB (bound to
 267 carbonates), OX (bound to Fe-Mn oxides), OM (bound to organic matter) and RS (residual) soil
 268 fractions. For each type of nanoparticle, bars with the same letter do not differ significantly (p
 269 < 0.05).

270
 271 The results show that the application of Fe-based NPs, nZVI and nGoethite, to this industrial
 272 brownfield site significantly reduced the availability of As in the soil, as revealed by the TCLP

273 test and the Tessier method. The effectiveness of the As immobilization depends on the dose
 274 of NPs used, although doses of nZVI higher than 5%, as seen in previous studies (Gil-Díaz et al.,
 275 2017a, 2016a, 2014), and 1% of nGoethite did not show higher efficiency. The best
 276 stabilization results were obtained with nGoethite, even at the lowest dose tested (0.2%). The
 277 As immobilization capacity of this nanomaterial at such a low dose is a critical factor when
 278 considering field-scale remediation.

279 3.3.2 Impact on As speciation

280 The As speciation analysis in the original soil revealed that the predominant form of As (>96%)
 281 was arsenate (As^{5+}), whereas arsenite (As^{3+}) was below 4%. The reduction of As^{5+} to As^{3+}
 282 species by nZVI was reported by Ramos et al. 2009 in water samples under anaerobic
 283 conditions, although in previous studies with As-polluted soils (Gil-Díaz et al., 2017a, 2016a,
 284 2014), this reduction was not been detected. In our case, the addition of nZVI at the highest
 285 dose caused a minor but significant increase of 1.4% in As^{3+} (arsenite) proportion, a more
 286 mobile and phytotoxic form compared to As^{5+} (arsenate) (Table 1). Nevertheless, as shown
 287 above, As immobilization by adsorption onto iron oxides in the outer layer of the NPs reduced
 288 As availability, as measured by the TCLP test and Tessier extracts. Therefore, the main process
 289 involved in the immobilization of As was arsenate adsorption, although a reduction process
 290 was also present but to a minor extent, which can be explained by the core-shell structure of
 291 nZVI. On the other hand, the reduction mechanism was not observed when nGoethite was
 292 tested; i.e., no changes in speciation were observed (Table 1). This observation points to an
 293 additional advantage of nGoethite over nZVI under the experimental conditions tested.

294 **Table 1.** Arsenic speciation results for untreated samples and samples treated at the highest
 295 dose (D4). For each type of nanoparticle, data with the same letter do not differ significantly (p
 296 < 0.05). **Note that mass recovery of the digestion method used is approximately 25% below of**
 297 **that obtained with aqua regia digestion.**

Sample	As(III)	As(V)
Control	3.8±0.1a	96.2±0.1a
nZVI	5.2±0.6b	94.8±0.6b

nGoethite	3.5±0.1a	96.5±0.1a
-----------	----------	-----------

298

299 3.3.3 Impact on the pH and EC of soil

300 Given the different chemical nature of the two types of NPs applied and the differences of pH
 301 in the suspensions (the nZVI suspension was alkaline, while the nGoethite suspension was
 302 acidic), we examined their effects at a range of dosages on soil pH and EC.

303 The data are shown in Table S2. **The application of nZVI did not affect pH or EC at any of the**
 304 **doses tested.** However, nGoethite addition at the highest dose led to a significant decrease of
 305 pH, falling from 8.23 to 7.38. A lower pH enhances As immobilization. In relation to EC soil
 306 values, nGoethite induced a notable increase, ranging from 0.55 dS m⁻¹ at the lowest dose to
 307 5.38 dS m⁻¹ at the highest one. This increase should be taken into account from the point of
 308 view of soil functionality, as the highest dose (D4) will impair the biological activity of the soil
 309 and plant development. **As immobilization was almost completed at moderate doses, thus it is**
 310 **suggested that the notable EC increase in doses D3 and especially in D4, is probably caused by**
 311 **an excess of nGoethite nanoparticles.**

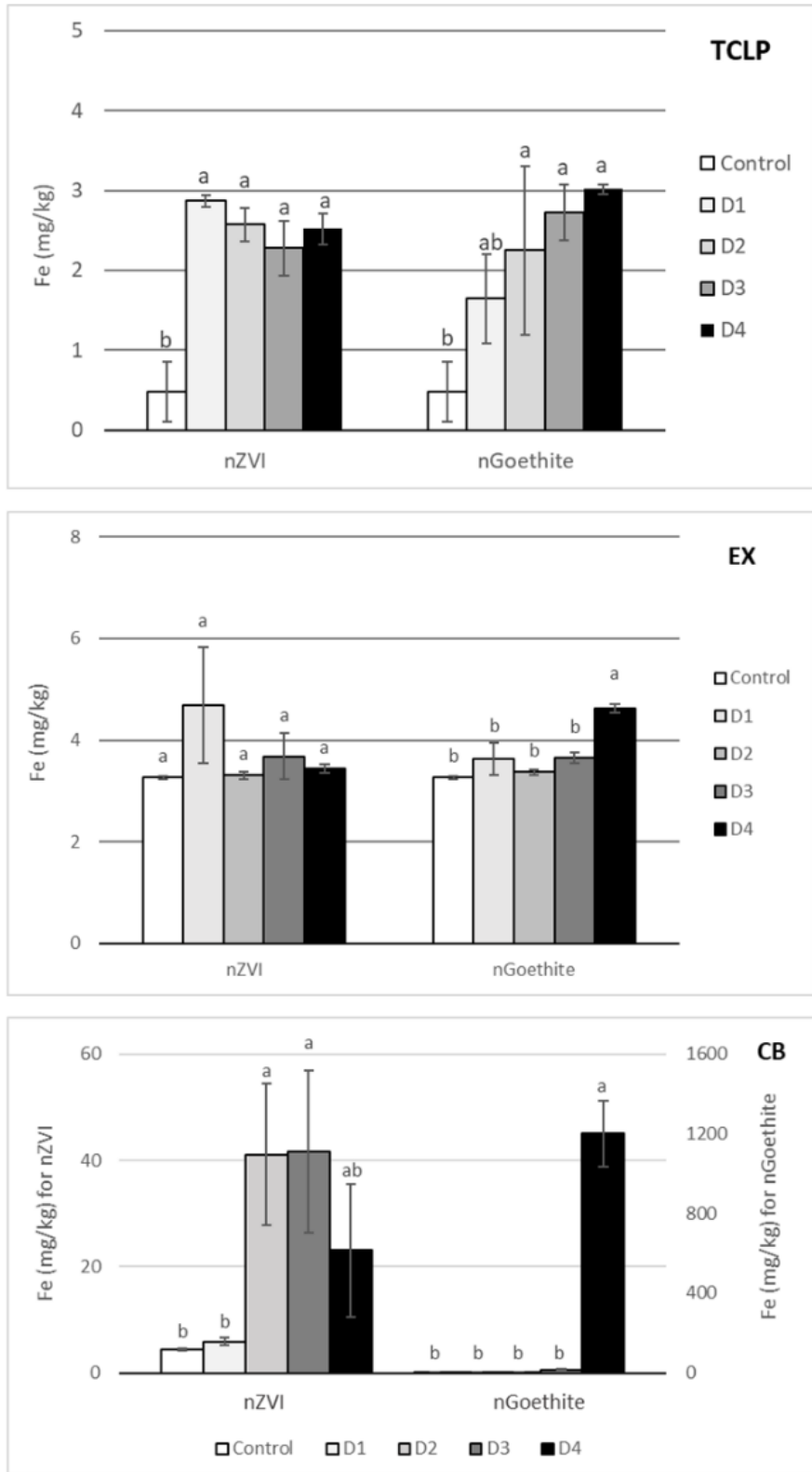
312 **Table 2.** Mean values and standard deviation of pH and electrical conductivity of soil samples
 313 treated with nZVI and nGoethite nanoparticles. For each type of nanoparticle, data with the
 314 same letter do not differ significantly (p < 0.05).

Treatment	Dose	pH	EC (dS/m)
Control	0%	8.23±0.04a	0.28±0.01a
nZVI	D1	8.58±0.10a	0.26±0.01a
	D2	8.48±0.09a	0.30±0.01a
	D3	8.63±0.11a	0.37±0.01b
	D4	9.05±0.20a	0.46±0.01c
nGoethite	D1	8.02±0.03ab	0.55±0.01b
	D2	8.00±0.09ab	1.56±0.02c
	D3	8.56±0.11a	2.43±0.07d
	D4	7.38±0.09b	5.38±0.03e

315

316 3.3.4 Impact on Fe availability

317 To determine the quantitative impact of the NP treatments on the availability of Fe in the soil,
 318 Fe concentration was measured. The Fe distribution in the TCLP extracts and in the most
 319 available Tessier fractions are showed in Figure 4.



320

321 **Figure 4.** Average concentration of iron (mg/kg) in TCLP extracts and in the EX (exchangeable)
322 and CB (bound to carbonates) soil fractions of the Tessier procedure. For each type of
323 nanoparticle, bars with the same letter do not differ significantly ($p < 0.05$).

324

325 The TCLP tests showed a slight increase in available Fe in all the treatments compared with
326 untreated soil. The increase was not dose-dependent.

327 Regarding the most available Tessier fractions, the addition of both types of NPs revealed a
328 different behavior.

329 The concentration of Fe in the EX fraction did not show significant variations for either type of
330 NP, with the exception of nGoethite treatment at the highest dose, which caused an increase
331 of 42%. This increase could be due to the extremely high dose; i.e., the Fe that has not reacted
332 with As and other soil components is in an available form.

333 In the CB fraction, Fe concentration increased between 430% and -856% in the nZVI treatment
334 at D2, D3 and D4. In the case of nGoethite treatment, no variation was observed in the CB
335 fraction, with the exception of the highest dose, in which a marked increase was detected,
336 probably attributable to the same reason as the increase in the EX fraction referred to above.

337 In summary, Fe is normally associated with the non-available fractions of Tessier extracts (Gil-
338 Díaz et al., 2016a, 2014). Therefore, in this case, it is particularly relevant that very small
339 differences and very low increases in Fe availability were observed for low doses of both nZVI
340 and nGoethite. However, medium and high doses of nZVI and the highest dose of nGoethite
341 led to a notable increase in the Fe bound to the CB fraction, and also to the EX fraction for
342 nGoethite.

343 *3.3.5 Soil phytotoxicity*

344 The results of the phytotoxicity assay are shown in Figure 5. According to Zucconi et al. (1985),
345 GI values below 50% indicate high phytotoxicity, between 50% and 80% moderate
346 phytotoxicity, and above 80% no phytotoxicity.

347 Initially, the untreated soil was highly phytotoxic to watercress since the GI of these plants was
348 <50%. The application of nZVI at all the doses tested significantly reduced phytotoxicity. These
349 results are consistent with those obtained from the sequential extraction procedure and TCLP
350 tests, which showed that treated soils showed a lower availability of As, the only contaminant
351 in the soil. The same effect was observed with the lowest dose of nGoethite, but not with the
352 higher ones. The latter observation can be explained by the dramatic increase in soil EC when
353 high amounts of nGoethite are added, as described above.

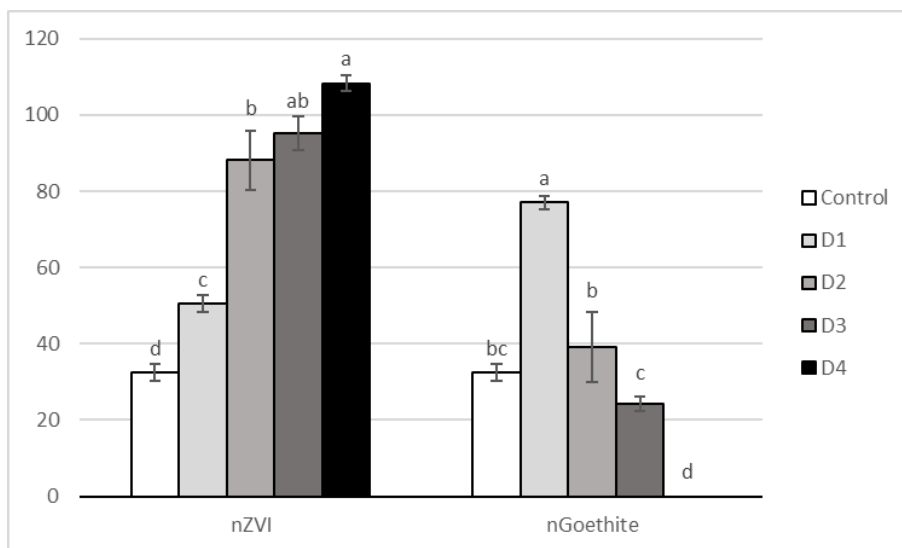


Figure 5. Mean germination index (%) of watercress for the soils treated with different doses of nanoparticles. For each type of nanoparticle, bars with the same letter do not differ significantly ($p < 0.05$).

354

355 **4. Conclusions**

356 The application of nZVI and nGoethite to soil samples from a brownfield polluted with As
357 caused a marked reduction in the availability of this heavy metalloid. The effectiveness of the
358 immobilization was significantly higher for nGoethite. However, the marked effect of high
359 doses of this nGoethite on the EC and phytotoxicity of soil may limit the use of this

360 nanomaterial for remediation purposes. The highest dose of nZVI (10% w/w) tested was
361 observed to cause a slight increase in arsenate reduction to arsenite (lower than 2%).

362 Our results demonstrate that both nZVI and nGoethite, at the lowest doses assayed (0.5% and
363 0.2 %, respectively) are efficient, although the former showed poorer As immobilization yields,
364 as revealed by measurements of As availability in the EX and CB fractions of the Tessier
365 method and in TCLP extracts. Moderate doses of nZVI outperformed nGoethite with respect to
366 As immobilization. However, some of the harmful effects of the highest doses nZVI, as
367 mentioned above, particularly its capacity to cause a slight increase in Fe availability, could
368 affect the appropriateness of this product.

369 On the basis of our findings, we conclude that, at the lowest dose assayed (0.2%), nGoethite is
370 a safe and promising technique for As immobilization. Regarding nZVI, a dose of 2% would
371 show a similar result for the remediation of the brownfield. Pilot or real-scale studies are now
372 required to validate these conclusions in a range of soil types.

373

374 **Acknowledgments**

375 This work was supported by the research projects REHABILITA CTM2016-78222-C2-1-R
376 AEI/FEDER, UE), FP-16-NANOREMED (IMIDRA, Comunidad de Madrid, Spain), and CTM2016-
377 75894-P (MINECO).

378 We would like also to thank the Environmental Assay Unit and the Electronic Microscope of
379 the Scientific and Technical Services of the University of Oviedo for technical support. Diego
380 Baragaño obtained a grant from the “Formación del Profesorado Universitario” program,
381 financed by the “Ministerio de Educación, Cultura y Deporte de España”.

382

383

384

385

386

387

388 **References**

389 **References**

390 Adriano, D.C., 2001. Trace Elements in Terrestrial Environments Biogeochemistry,
391 Bioavailability, and Risks of Metals, Volume I. <https://doi.org/10.1007/978-0-387-21510-5>

392 Aide, M., Beighley, D., Dunn, D., 2016. Arsenic In The Soil Environment : A Soil Chemistry
393 Review. *Int. J. Appl. Agric. Res.* 11, 1–28.

394 Alekseenko, V.A., Bech, J., Alekseenko, A. V., Shvydkaya, N. V., Roca, N., 2018. Environmental
395 impact of disposal of coal mining wastes on soils and plants in Rostov Oblast, Russia. *J.*
396 *Geochemical Explor.* 184, 261–270. <https://doi.org/10.1016/j.gexplo.2017.06.003>

397 Atkinson, R.J., Posner, A.M., Quirk, J.P., 1968. Crystal nucleation in Fe(III) solutions and
398 hydroxide gels. *J. Inorg. Nucl. Chem.* 30, 2371–2381. [https://doi.org/10.1016/0022-](https://doi.org/10.1016/0022-1902(68)80247-7)
399 [1902\(68\)80247-7](https://doi.org/10.1016/0022-1902(68)80247-7)

400 Baragaño, D., Rodríguez-Valdés, E., Peláez, A.I., Boente, C., Matanzas, N., García, N., Gallego,
401 J.L.R., 2018. Environmental Forensic Study and Remediation Feasibility in an Abandoned
402 Industrial Site. *Proceedings 2*, 1503. <https://doi.org/10.3390/proceedings2231503>

403 Boente, C., Matanzas, N., García-González, N., Rodríguez-Valdés, E., Gallego, J.R., 2017. Trace
404 elements of concern affecting urban agriculture in industrialized areas: A multivariate
405 approach. *Chemosphere* 183, 546–556.
406 <https://doi.org/10.1016/j.chemosphere.2017.05.129>

407 BOJA, Boletín Oficial de la Junta de Andalucía, 38, February 2015. Regulation that regulates the
408 regime applicable to contaminated soils.

409 https://www.juntadeandalucia.es/medioambiente/portal_web/web/temas_ambientales/suel
410 [o/suelos_contaminados/reglamento_suelos_contaminados.pdf](https://www.juntadeandalucia.es/medioambiente/portal_web/web/temas_ambientales/suel/o/suelos_contaminados/reglamento_suelos_contaminados.pdf) (Accessed February
411 2019).

412 Chen, Y.H., Li, F.A., 2010. Kinetic study on removal of copper(II) using goethite and hematite
413 nano-photocatalysts. *J. Colloid Interface Sci.* 347, 277–281.
414 <https://doi.org/10.1016/j.jcis.2010.03.050>

415 Davis, B.S., Birch, G.F., 2011. Spatial distribution of bulk atmospheric deposition of heavy
416 metals in metropolitan Sydney, Australia. *Water. Air. Soil Pollut.* 214, 147–162.
417 <https://doi.org/10.1007/s11270-010-0411-3>

418 Fajardo, C., Ortíz, L.T., Rodríguez-Membibre, M.L., Nande, M., Lobo, M.C., Martín, M., 2012.
419 Assessing the impact of zero-valent iron (ZVI) nanotechnology on soil microbial structure
420 and functionality: A molecular approach. *Chemosphere* 86, 802–808.
421 <https://doi.org/10.1016/j.chemosphere.2011.11.041>

422 Fajardo, C., Gil-Díaz, M., Costa, G., Alonso, J., Guerrero, A.M., Nande, M., Lobo, M.C., Martín,
423 M., 2015. Residual impact of aged nZVI on heavy metal-polluted soils. *Sci. Total Environ.*
424 535, 79–84. <https://doi.org/10.1016/j.scitotenv.2015.03.067>

425 Fendorf, S., Eick, M.J., Grossl, P., Sparks, D.L., 1997. Arsenate and chromate retention
426 mechanisms on goethite. 1. Surface structure. *Environ. Sci. Technol.* 31, 315–320.
427 <https://doi.org/10.1021/es950653t>

428 Forján, R., Asensio, V., Rodríguez-Vila, A., Covelo, E.F., 2016. Contribution of waste and biochar
429 amendment to the sorption of metals in a copper mine tailing. *Catena* 137, 120–125.
430 <https://doi.org/10.1016/j.catena.2015.09.010>

- 431 Fraga, C.G., Oteiza, P.I., Keen, C.L., 2005. Trace elements and human health. *Mol. Aspects Med.*
432 26, 233–234. <https://doi.org/10.1016/j.mam.2005.07.014>
- 433 Gallego, J.R., Ortiz, J.E., Sierra, C., Torres, T., Llamas, J.F., 2013. Multivariate study of trace
434 element distribution in the geological record of Roñanzas Peat Bog (Asturias, N. Spain).
435 Paleoenvironmental evolution and human activities over the last 8000calyr BP. *Sci. Total*
436 *Environ.* 454–455, 16–29. <https://doi.org/10.1016/j.scitotenv.2013.02.083>
- 437 Gallego, J.R., Rodríguez-Valdés, E., Esquinas, N., Fernández-Braña, A., Afif, E., 2016. Insights
438 into a 20-ha multi-contaminated brownfield megasite: An environmental forensics
439 approach. *Sci. Total Environ.* 563–564, 683–692.
440 <https://doi.org/10.1016/j.scitotenv.2015.09.153>
- 441 Gao, S., Goldberg, S., Herbel, M.J., Chalmers, A.T., Fujii, R., Tanji, K.K., 2006. Sorption processes
442 affecting arsenic solubility in oxidized surface sediments from Tulare Lake Bed, California.
443 *Chem. Geol.* 228, 33–43. <https://doi.org/10.1016/j.chemgeo.2005.11.017>
- 444 Gil-Díaz, M., Alonso, J., Rodríguez-Valdés, E., Pinilla, P., Lobo, M.C., 2014. Reducing the mobility
445 of arsenic in brownfield soil using stabilised zero-valent iron nanoparticles. *J. Environ. Sci.*
446 *Heal. - Part A Toxic/Hazardous Subst. Environ. Eng.* 49, 1361–1369.
447 <https://doi.org/10.1080/10934529.2014.928248>
- 448 Gil-Díaz, M., Diez-Pascual, S., González, A., Alonso, J., Rodríguez-Valdés, E., Gallego, J.R., Lobo,
449 M.C., 2016a. A nanoremediation strategy for the recovery of an As-polluted soil.
450 *Chemosphere* 149, 137–145. <https://doi.org/10.1016/j.chemosphere.2016.01.106>
- 451 Gil-Díaz, M., González, A., Alonso, J., Lobo, M.C., 2016b. Evaluation of the stability of a
452 nanoremediation strategy using barley plants. *J. Environ. Manage.* 165, 150–158.
453 <https://doi.org/10.1016/j.jenvman.2015.09.032>
- 454 Gil-Díaz, M., Alonso, J., Rodríguez-Valdés, E., Gallego, J.R., Lobo, M.C., 2017a. Comparing

455 different commercial zero valent iron nanoparticles to immobilize As and Hg in
456 brownfield soil. *Sci. Total Environ.* 584–585, 1324–1332.
457 <https://doi.org/10.1016/j.scitotenv.2017.02.011>

458 Gil-Díaz, M., Pinilla, P., Alonso, J., Lobo, M.C., 2017b. Viability of a nanoremediation process in
459 single or multi-metal(loid) contaminated soils. *J. Hazard. Mater.* 321, 812–819.
460 <https://doi.org/10.1016/j.jhazmat.2016.09.071>

461 Gil-Díaz, M., Lobo, M.C. 2018. Phytotoxicity of Nanoscale Zerovalent Iron (nZVI) in Remediation
462 Strategies in: *Phytotoxicity of Nanoparticles*. M. Faisal et al. (eds.), Springer International
463 Publishing AG, part of Springer Nature 2018. [https://doi.org/10.1007/978-3-319-76708-](https://doi.org/10.1007/978-3-319-76708-6_13)
464 [6_13](https://doi.org/10.1007/978-3-319-76708-6_13)

465 Gil-Díaz, M., Rodríguez-Valdés, E., Alonso, J., Baragaño, D., Gallego, J.R., Lobo, M.C. 2019.
466 Nanoremediation and long-term monitoring of brownfield soil highly polluted with As
467 and Hg. *Sci. Total Environ.* 675, 165-175. <https://doi.org/10.1016/j.scitotenv.2019.04.183>

468 Giménez, J., Martínez, M., de Pablo, J., Rovira, M., Duro, L., 2007. Arsenic sorption onto natural
469 hematite, magnetite, and goethite. *J. Hazard. Mater.* 141, 575–580.
470 <https://doi.org/10.1016/j.jhazmat.2006.07.020>

471 Gonçalves, J.R., 2016. The Soil and Groundwater Remediation with Zero Valent Iron
472 Nanoparticles, in: *Procedia Engineering*. pp. 1268–1275.
473 <https://doi.org/10.1016/j.proeng.2016.06.122>

474 González, A., García- Gonzalo, P., Gil-Díaz, M., Alonso, J., Lobo, M.C., 2019. Compost-assisted
475 phytoremediation of As-polluted soil. *Journal of Soils and Sediments*.
476 <https://doi.org/10.1007/s11368-019-02284-9>

477 Gopalakrishnan, A., Krishnan, R., Thangavel, S., Venugopal, G., Kim, S.J., 2015. Removal of
478 heavy metal ions from pharma-effluents using graphene-oxide nanosorbents and study of

479 their adsorption kinetics. *J. Ind. Eng. Chem.* 30, 14–19.
480 <https://doi.org/10.1016/j.jiec.2015.06.005>

481 Hartley, W., Edwards, R., Lepp, N.W., 2004. Arsenic and heavy metal mobility in iron oxide-
482 amended contaminated soils as evaluated by short- and long-term leaching tests.
483 *Environ. Pollut.* 131, 495–504. <https://doi.org/10.1016/j.envpol.2004.02.017>

484 Hartley, W., Lepp, N.W., 2008. Remediation of arsenic contaminated soils by iron-oxide
485 application, evaluated in terms of plant productivity, arsenic and phytotoxic metal
486 uptake. *Sci. Total Environ.* 390, 35–44. <https://doi.org/10.1016/j.scitotenv.2007.09.021>

487 Hasegawa, H., Rahman, I.M.M., Rahman, M.A., 2015. Environmental Remediation
488 Technologies for Metal-Contaminated Soils, *Environmental Remediation Technologies for*
489 *Metal-Contaminated Soils*. <https://doi.org/10.1007/978-4-431-55759-3>

490 Hopkins, J., Watts, P., Hosford, M., 2009. Contaminants in soil: updated collation of
491 toxicological data and intake values for humans Inorganic arsenic. Science report:
492 SC050021/TOX 1. Environment Agency.
493 [http://webarchive.nationalarchives.gov.uk/20140328084622/http://www.environment-](http://webarchive.nationalarchives.gov.uk/20140328084622/http://www.environment-agency.gov.uk/research/planning/64002.aspx)
494 [agency.gov.uk/research/planning/64002.aspx](http://www.environment-agency.gov.uk/research/planning/64002.aspx) (Accessed February 2019).

495 Hua, M., Zhang, S., Pan, B., Zhang, W., Lv, L., Zhang, Q., 2012. Heavy metal removal from
496 water/wastewater by nanosized metal oxides: A review. *J. Hazard. Mater.*
497 <https://doi.org/10.1016/j.jhazmat.2011.10.016>

498 Irem, S., Islam, E., Maathuis, F.J.M., Niazi, N.K., Li, T., 2019. Assessment of potential dietary
499 toxicity and arsenic accumulation in two contrasting rice genotypes: Effect of soil
500 amendments. *Chemosphere* 225, 104–114.
501 <https://doi.org/10.1016/j.chemosphere.2019.02.202>

502 Khalid, S., Shahid, M., Niazi, N.K., Murtaza, B., Bibi, I., Dumat, C., 2017. A comparison of

503 technologies for remediation of heavy metal contaminated soils. *J. Geochemical Explor.*
504 182, 247–268. <https://doi.org/10.1016/j.gexplo.2016.11.021>

505 Kim, K.R., Lee, B.T., Kim, K.W., 2012. Arsenic stabilization in mine tailings using nano-sized
506 magnetite and zero valent iron with the enhancement of mobility by surface coating. *J.*
507 *Geochemical Explor.* 113, 124–129. <https://doi.org/10.1016/j.gexplo.2011.07.002>

508 Klimkova, S., Cernik, M., Lacinova, L., Filip, J., Jancik, D., Zboril, R., 2011. Zero-valent iron
509 nanoparticles in treatment of acid mine water from in situ uranium leaching.
510 *Chemosphere* 82, 1178–1184. <https://doi.org/10.1016/j.chemosphere.2010.11.075>

511 Komárek, M., Vaněk, A., Ettler, V., 2013. Chemical stabilization of metals and arsenic in
512 contaminated soils using oxides - A review. *Environ. Pollut.*
513 <https://doi.org/10.1016/j.envpol.2012.07.045>

514 Kumpiene, J., Lagerkvist, A., Maurice, C., 2008. Stabilization of As, Cr, Cu, Pb and Zn in soil
515 using amendments - A review. *Waste Manag.* 28, 215–225.
516 <https://doi.org/10.1016/j.wasman.2006.12.012>

517 Lado, L.R., Hengl, T., Reuter, H.I., 2008. Heavy metals in European soils: A geostatistical analysis
518 of the FOREGS Geochemical database. *Geoderma* 148, 189–199.
519 <https://doi.org/10.1016/j.geoderma.2008.09.020>

520 Laumann, S., Micić, V., Lowry, G. V., Hofmann, T., 2013. Carbonate minerals in porous media
521 decrease mobility of polyacrylic acid modified zero-valent iron nanoparticles used for
522 groundwater remediation. *Environ. Pollut.* 179, 53–60.
523 <https://doi.org/10.1016/j.envpol.2013.04.004>

524 Li, Z., Greden, K., Alvarez, P.J.J., Gregory, K.B., Lowry, G. V., 2010. Adsorbed polymer and NOM
525 limits adhesion and toxicity of nano scale zerovalent iron to *E. coli*. *Environ. Sci. Technol.*
526 44, 3462–3467. <https://doi.org/10.1021/es9031198>

527 Cagigal, E., Ocejo, M., Gallego, J.R., Peláez, A.I., Rodríguez-Valdés, E., 2018. Environmental
528 Effects of the Application of Iron Nanoparticles for Site Remediation, in: Iron
529 Nanomaterials for Water and Soil Treatment. pp. 283–307.
530 <https://doi.org/10.1201/b22501-12>

531 Magiera, T., Zawadzki, J., Szuszkiewicz, M., Fabijańczyk, P., Steinnes, E., Fabian, K., Miszczak, E.,
532 2018. Impact of an iron mine and a nickel smelter at the Norwegian/Russian border close
533 to the Barents Sea on surface soil magnetic susceptibility and content of potentially toxic
534 elements. *Chemosphere* 195, 48–62.
535 <https://doi.org/10.1016/j.chemosphere.2017.12.060>

536 MAPA, 1994. Métodos Oficiales de Análisis. Secretaría General Técnica Ministerio de
537 Agricultura, Pesca y Alimentación, Madrid. vol. III, pp. 219–324.

538 Marker, B.R., 2018. Brownfield Sites. pp. 92–94. [https://doi.org/10.1007/978-3-319-73568-](https://doi.org/10.1007/978-3-319-73568-9_36)
539 [9_36](https://doi.org/10.1007/978-3-319-73568-9_36)

540 Mesa, V., Navazas, A., González-Gil, R., González, A., Weyens, N., Lauga, B., Gallego, J.R.,
541 Sánchez, J., Peláez, A.I., 2017. Use of Endophytic and Rhizosphere Bacteria To Improve
542 Phytoremediation of Arsenic-Contaminated Industrial Soils by Autochthonous *Betula*
543 *celtiberica*. *Appl. Environ. Microbiol.* 83. <https://doi.org/10.1128/aem.03411-16>

544 Mueller, N.C., Braun, J., Bruns, J., Černík, M., Rissing, P., Rickerby, D., Nowack, B., 2012.
545 Application of nanoscale zero valent iron (NZVI) for groundwater remediation in Europe.
546 *Environ. Sci. Pollut. Res.* 19, 550–558. <https://doi.org/10.1007/s11356-011-0576-3>

547 O’Carroll, D., Sleep, B., Krol, M., Boparai, H., Kocur, C., 2013. Nanoscale zero valent iron and
548 bimetallic particles for contaminated site remediation. *Adv. Water Resour.* 51, 104–122.
549 <https://doi.org/10.1016/j.advwatres.2012.02.005>

550 O’Reilly, S.E., Strawn, D.G., Sparks, D.L., 2010. Residence Time Effects on Arsenate

551 Adsorption/Desorption Mechanisms on Goethite. *Soil Sci. Soc. Am. J.* 65, 67.
552 <https://doi.org/10.2136/sssaj2001.65167x>

553 Pérez-Sanz, A., Vázquez, S., Lobo, M.C., Moreno-Jimenez, E., García, P., Carpena, R.O., 2013.
554 Soil Factor controlling arsenic availability for *Silene vulgaris*. *Commun. Soil Sci. Plan.*
555 44(1414), 2152-2167. <https://doi.org/10.1080/00103624.2013.799683>

556 Rahimi, S., Moattari, R.M., Rajabi, L., Derakhshan, A.A., Keyhani, M., 2015. Iron
557 oxide/hydroxide (α,γ -FeOOH) nanoparticles as high potential adsorbents for lead removal
558 from polluted aquatic media. *J. Ind. Eng. Chem.* 23, 33–43.
559 <https://doi.org/10.1016/j.jiec.2014.07.039>

560 Rahmani, A.R., Ghaffari, H.R., Samadi, M.T., 2010. Removal of Arsenic (III) from Contaminated
561 Water by Synthetic Nano Size Zerovalent Iron. *World Acad. Sci. Eng. Technol.* 4, 647–650.

562 Rao, L.N., 2014. Environmental impact of uncontrolled disposal of e-wastes. *Int. J. ChemTech*
563 *Res.* 6, 1343–1353.

564 Saccà, M.L., Fajardo, C., Costa, G., Lobo, C., Nande, M., Martin, M., 2014. Integrating classical
565 and molecular approaches to evaluate the impact of nanosized zero-valent iron (nZVI) on
566 soil organisms. *Chemosphere* 104, 184–189.
567 <https://doi.org/10.1016/j.chemosphere.2013.11.013>

568 Santucci, L., Carol, E., Tanjal, C., 2018. Industrial waste as a source of surface and groundwater
569 pollution for more than half a century in a sector of the Río de la Plata coastal plain
570 (Argentina). *Chemosphere* 206, 727–735.
571 <https://doi.org/10.1016/j.chemosphere.2018.05.084>

572 Schmid, D., Micić, V., Laumann, S., Hofmann, T., 2015. Measuring the reactivity of
573 commercially available zero-valent iron nanoparticles used for environmental
574 remediation with iopromide. *J. Contam. Hydrol.* 181, 36–45.

575 <https://doi.org/10.1016/j.jconhyd.2015.01.006>

576 Siddiqui, S.I., Chaudhry, S.A., 2018. A review on graphene oxide and its composites preparation
577 and their use for the removal of As³⁺ and As⁵⁺ from water under the effect of various
578 parameters: Application of isotherm, kinetic and thermodynamics. *Process Saf. Environ.*
579 *Prot.* <https://doi.org/10.1016/j.psep.2018.07.020>

580 Singh, R., Misra, V., 2015. Stabilization of zero-valent iron nanoparticles: role of polymers and
581 surfactants. *Handbook of nanoparticles*. Springer, [https://doi.org/10.1007/978-3-319-](https://doi.org/10.1007/978-3-319-13188-7_44-2)
582 [13188-7_44-2](https://doi.org/10.1007/978-3-319-13188-7_44-2)

583 Tessier, A., Campbell, P.G.C., Bisson, M., 1979. Sequential Extraction Procedure for the
584 Speciation of Particulate Trace Metals. *Anal. Chem.* 51, 844–851.
585 <https://doi.org/10.1021/ac50043a017>

586 Waychunas, G.A., Kim, C.S., Banfield, J.F., 2005. Nanoparticulate iron oxide minerals in soils
587 and sediments: Unique properties and contaminant scavenging mechanisms, in: *Journal*
588 *of Nanoparticle Research*. pp. 409–433. <https://doi.org/10.1007/s11051-005-6931-x>

589 Zhang, M.Y., Wang, Y., Zhao, D.Y., Pan, G., 2010. Immobilization of arsenic in soils by stabilized
590 nanoscale zero-valent iron, iron sulfide (FeS), and magnetite (Fe₃O₄) particles. *Chinese*
591 *Sci. Bull.* 55, 365–372. <https://doi.org/10.1007/s11434-009-0703-4>

592 Zucconi, F., Monaco, A., Forte, M., De Bertoldi, M., 1985. Phytotoxins during the stabilization
593 of organic matter, in: *Composting of Agricultural and Other Wastes*. pp. 73–86.

594

Supplementary Material

[Click here to download Supplementary Material: Baragao et al 2019 supplementary revised manuscript.docx](#)

1 **Zero valent iron and goethite nanoparticles as new promising** 2 **remediation techniques for As-polluted soils**

3 D. Baragaño^a, J. Alonso^b, J.R. Gallego^a, M.C. Lobo^b, M. Gil-Díaz^b

4 ^a INDUROT, Environmental Technology, Biotechnology, and Geochemistry Group, Universidad
5 de Oviedo, Campus de Mieres, 33600 Mieres, Asturias, Spain

6 ^b IMIDRA, Instituto Madrileño de Investigación y Desarrollo Rural, Agrario y Alimentación, Finca
7 “El Encín”, Alcalá de Henares, 28800, Madrid, Spain

8 **Abstract**

9 The capacity of two iron-based nanomaterials, namely goethite nanospheres (nGoethite) and
10 zero valent iron nanoparticles (nZVI), to immobilize As in a polluted soil was evaluated and
11 compared. The composition and morphology of the products were studied by energy
12 dispersive X-ray analysis and transmission electron microscopy, while zeta potential and
13 average sizes were determined by dynamic light scattering. To assess As immobilization, soil
14 subsamples were treated with nGoethite or nZVI at a range of Fe doses (0.5%, 2%, 5% and
15 10%) and then studied by the TCLP test and the Tessier sequential extraction procedure. The
16 influence of both nanoparticles on As speciation was determined, as was impact on soil pH,
17 electrical conductivity, Fe availability and phytotoxicity (watercress germination). For nZVI,
18 notable results were achieved at a dose of 2% (89.5% decrease in As, TCLP test), and no
19 negative effects on soil parameters were detected. Indeed, even soil phytotoxicity was
20 reduced and only at the highest dose was a slight increase in As³⁺ detected. In contrast,
21 excellent results were obtained for nGoethite at the lowest dose (0.2%) (82.5% decrease in As,
22 TCLP test); however, soil phytotoxicity was increased at higher doses, probably due to a
23 marked enhancement of electrical conductivity. For both types of nanoparticle, slight increases
24 in Fe availability were observed. Thus, our results show that both nZVI and nGoethite have the
25 capacity to effectively immobilize As in this brownfield. The use of lower doses of nGoethite
26 emerges as a promising soil remediation strategy for soils affected by As pollution.

27 **Keywords**

28 Arsenic; soil pollution; nZVI; goethite nanoparticles; immobilization; brownfield

29 **1. Introduction**

30 The closure of industrial and mining facilities has brought to light the presence of large
31 volumes of contaminated soil worldwide (Adriano, 2001; Gallego et al., 2016; Santucci et al.,
32 2018). These sites, known as brownfields (Marker, 2018), are particularly common in areas
33 with a history of heavy industrial activity. Among the pollutants found in brownfield soils,
34 Potentially Toxic Elements (PTEs), such as Pb, As, Cu or Zn, are some of the most frequent due
35 to their release during industrial processes (Lado et al., 2008; Magiera et al., 2018),
36 atmospheric deposition (Boente et al., 2017; Davis and Birch, 2011) and inappropriate
37 dumping of waste (Alekseenko et al., 2018; Rao, 2014). PTEs, even at low concentrations, can
38 pose a serious threat to human health and ecosystems (Fraga et al., 2005; Gopalakrishnan et
39 al., 2015; Irem et al., 2019).

40 In particular, arsenic (As) is a highly toxic and carcinogenic element and as such it compromises
41 ecosystem quality and human health (Hopkins et al., 2009). In general, As(V) and As(III) are the
42 most common stable oxidation states of this heavy metal in soils (Aide et al., 2016),
43 As(III) being more toxic than As(V). Classical methods for the remediation of As-contaminated
44 soils require physical/chemical methods such as solidification/stabilization, soil washing, and
45 electrokinetics, or biological strategies such as phytoremediation (Forján et al., 2016; Gonzalez
46 et al., 2019; Hasegawa et al., 2015; Khalid et al., 2017; Kumpiene et al., 2008; Mesa et al., 2017;
47 Pérez-Sanz et al., 2013). Among the most common techniques used in situ, those based on
48 arsenate immobilization through adsorption and surface complexation on iron-based
49 compounds have been widely studied (Hartley et al., 2004; Hartley and Lepp, 2008; Chen and
50 Li, 2010; Komárek et al., 2013). Sorption on iron oxides was found to lead to inner-sphere
51 surface complexation, including monodentate, bidentate mononuclear, and bidentate
52 binuclear complexes (Fendorf et al., 1997; Gao et al., 2006; Hua et al., 2012; Rahimi et al.,
53 2015).

54 Recent years have witnessed the development of nanoremediation as a novel technique to
55 immobilize heavy metal(oid)s, especially methods involving the addition of nanoscale zero
56 valent iron nanoparticles (nZVI) to stabilize and reduce PTE availability (Gil-Diaz et al., 2017a,
57 2017b, 2019; Gonçalves, 2016; Mueller et al., 2012; O'Carroll et al., 2013). nZVI usually present
58 acicular shapes, thus increasing the specific surface of granular iron and achieving higher
59 reactivity due to their size (O'Carroll et al., 2013). Several studies have shown that nZVI
60 effectively immobilize As in water samples and soils (Gil-Díaz et al., 2017a; Kim et al., 2012;
61 Rahmani et al., 2010), even in field conditions (Gil-Díaz et al., 2019). In aqueous solutions, nZVI
62 react with water and oxygen to form an outer Fe (hydr)oxide layer, so these particles present
63 a core-shell structure (O'Carroll et al., 2013). In this context, differences in the structural
64 properties of nZVI strongly influence the reactivity and aging of the particles (Fajardo et al.,
65 2015; Gil-Díaz et al., 2017b, 2016a). In addition, risks due to the potential toxicity of nZVI have
66 been reported and should be taken into account (Cagigal et al., 2018; Gil-Diaz and Lobo, 2018).
67 In this regard, nanoparticle (NP) dose, exposure time, oxidation rate and Fe availability are
68 parameters to be considered (Fajardo et al., 2012; Gil-Diaz et al., 2017b; Li et al., 2010; Saccà
69 et al., 2014).

70 To overcome these difficulties, other NPs based on Fe oxides have been used for
71 environmental remediation purposes. In this regard, they have shown greater stability than
72 nZVI when used for PTE removal from water (Chen and Li, 2010; Rahimi et al., 2015) or even
73 from soils (Waychunas et al., 2005; Zhang et al., 2010). In particular, iron oxy-hydroxide (α -
74 FeOOH) is a natural oxide mineral, known as goethite, which promotes contaminant
75 sequestration (including As) by sorption processes (Giménez et al., 2007; Waychunas et al.,
76 2005). Indeed, even synthetic goethite has been produced (Atkinson et al., 1968) and applied
77 for As immobilization (O'Reilly et al., 2010). In this context, synthesized goethite have recently
78 been used successfully to remove Cu and Pb from polluted water, achieving better results than
79 other iron oxides (Chen and Li, 2010; Rahimi et al., 2015). However, to the best of our

80 knowledge, despite the great potential of goethite as an adsorbent, the capacity of goethite
81 NPS (nGoethite) to remove As from water or immobilize As in soils has not been tested.

82 The main objectives of this work are: i) to compare the effectiveness of commercial nZVI and
83 nGoethite to immobilize As in an industrial polluted soil; and ii) to determine potential toxic
84 effects of these nanoparticles by means of Fe availability and soil phytotoxicity evaluation.

85 **2. Materials and methods**

86 **2.1 Samples**

87 Samples were taken from polluted soils in one of the main former fertilizer plants in southern
88 Spain (Andalusia), which operated for almost forty years until its closure in 1997. Following its
89 dismantling in 2001, characterization studies revealed areas with concentrations of As
90 exceeding soil screening levels (Baragaño et al., 2018).

91 Within the area affected by As pollution, a 5-kg composite soil sample was collected from the
92 surface layer (0 – 25 cm) with a manual auger. It was then air-dried, homogenized and sieved
93 (<2 mm) prior to analysis.

94 **2.2 Analyses**

95 The physico-chemical properties of the soil were determined in representative subsamples
96 using the Spanish official methodology (MAPA, 1994). In brief, organic matter was determined
97 using the Walkley-Black method (dichromate oxidation); pH and electrical conductivity (EC)
98 were measured in a 1:2.5 soil-to-water ratio; total nitrogen content was quantified by the
99 Kjeldahl method; the percentage of carbonates was measured using a Bernard calcimeter; and
100 available nutrients (Ca, K, Mg, Na) were extracted with 0.1 N ammonium acetate and
101 quantified using a flame atomic absorption spectrometer (AA240FS, Varian). Grain size was
102 characterized by wet-sieving and laser diffraction spectroscopy using the Aqueous Dry Module
103 of an LS 13 320MW system (Beckman Inc. Coulter).

104 Pseudo-total metal(loid) concentrations were determined after acid digestion with a mixture
105 of 6 mL nitric acid (69% purity) and 2 mL of hydrochloric acid (37% purity), in a microwave
106 reaction system (Multiwave Go, Anton Paar GmbH). In the digestion extract, the
107 concentrations of Fe, Cd, Cr, Cu, Ni, Pb and Zn were quantified by flame atomic absorption
108 spectrometry (FAAS) (AA240FS, Varian) and As by graphite furnace atomic absorption
109 spectrometry (GFAAS) with Zeeman Correction (AA240Z, Varian).

110 **2.3 Iron-based nanoparticles characterization**

111 Two types of commercially iron NPs were purchased: Zero valent iron NPs (nZVI) called
112 NANOFER 25S, obtained from Nano Iron s.r.o., (Rajhrad, Czech Republic), and goethite NPs
113 (nGoethite) synthesized by Cerion Advanced Materials (USA) and obtained from Sigma-Aldrich
114 (USA, #796093). The NPs were used immediately after receipt, thereby preventing any
115 chemical alteration, and solutions were covered with aluminium foil to prevent light-induced
116 degradation.

117 Chemical and macro-morphology studies of both types of NP were performed by scanning-
118 electron microscope and energy dispersive X-ray spectroscopy (SEM-EDX) using a JEOL JSM-
119 5600 Scanning Electron Microscope coupled to an Energy Dispersive X-ray analyzer (INCA
120 Energy 200).

121 The size and morphology of the NPs were measured in a JEOL JEM-2100F transmission electron
122 microscope (TEM). For TEM observations, sample preparation involved the dispersion of the
123 NPs in a suspension of water by means of sonication, and deposition on a holey carbon film-
124 coated copper grid and subsequent drying. The mean size of NPs was determined by image
125 analysis and confirmed by dynamic light scattering (DLS) using a Zetasizer Nano ZS (Malvern
126 Panalytical). Finally, to determine surface charge and given that the sorption mechanism
127 between As and iron oxides is a surface phenomenon, the zeta potential of the NPs was
128 determined using a Zetasizer Nano ZS.

129 **2.4 Batch experiments and monitoring**

130 To test the effectiveness of the NPs for As immobilization, 20-g subsamples of polluted soil
131 were treated with each type of NP at different doses in 50-mL plastic vials. nZVI doses of 0.5%,
132 2%, 5% and 10% (w:w) were selected on the basis of previous studies with other As-polluted
133 soils (Gil-Díaz et al., 2017a, 2017b, 2016a). nGoethite doses of 0.2%, 1%, 2% and 5% were
134 selected in order to facilitate comparison of the effects of the two distinct types of NPs at a
135 similar Fe content per gram of soil, i.e., the amount of Fe added to the soil corresponded to
136 that of the nZVI experiments. Therefore increasing doses of Fe are labeled henceforth as D1,
137 D2, D3 and D4 irrespective of the NPs used.

138 Before beginning the experiments, deionized water was added to the soil samples to achieve
139 water holding capacity in order to improve nanoparticles and soil contact. NPs were then
140 applied, except for control tests, which were treated only with deionized water. Experiments
141 were carried out in triplicate. Vials were shaken for 72 h at 100 rpm in a Reax 2 shaker
142 (Heidolph Instrument GmbH & Co. KG). After shaking, samples were air dried.

143 To quantify potential As leachability, the TCLP test (Toxicity Characteristic Leaching Procedure)
144 was performed following the USEPA Method 1311 (1992). Furthermore, to determine the
145 potential mobility and availability of As in soil samples, the sequential extraction procedure
146 proposed by Tessier et al. (1979) was also performed. In brief, extracts with reagents of
147 increasing strengths were sequentially added to the subsamples. The following fractions were
148 obtained: exchangeable (EX); bound to carbonates (CB); bound to Fe-Mn oxides (OX); bound to
149 organic matter (OM); and residual (RS). As and Fe concentrations were measured in the
150 extracts following the methodology described in section 2.2. Electrical conductivity (EC) and pH
151 were also measured to evaluate the influence of NP application on soil properties in a
152 suspension of soil and distilled water (1:2.5).

153 For measuring As species, 0.1 g of soil and 15 mL of the extracting agent (1 M H₃PO₄ + 0.1 M
154 ascorbic acid) were placed in a microwave vessel and digested (Multiwave 3000, Anton Paar
155 GmbH) at 60W for 10 min (Garcia-Manyes et al., 2002). After cooling, the extracts were diluted
156 and filtered (0.45 µm). The As species were separated in a 4.6 mm x 150 mm As Separation
157 Column (Agilent Technologies) fitted to a 1260 Infinity HPLC coupled to a 7700 ICP-MS (Agilent
158 Technologies) using a mobile phase of 2 M PBS (Phosphate Buffered Saline)/0.2 M EDTA (pH =
159 6.0) at a flow of 1 mL/min.

160 **2.5 Soil phytotoxicity**

161 The phytotoxicity of the NP-treated and untreated soil samples was determined using a
162 modified version of the Zucconi test (Zucconi et al., 1985), as described in a previous study (Gil-
163 Díaz et al., 2014). In brief, six watercress (*Nasturtium officinale*) seeds moistened with 6 mL of
164 distilled water (control) or soil extract were placed in triplicate Petri dishes. Soil extracts were
165 obtained by means of 5 g of air-dried in contact with 50 mL of distilled water at 60°C during 30
166 min, followed by filtering with a Whatman paper (541 grade). After two days of incubation in
167 the dark at 26-27°C, the seed germination percentage was calculated and the root length of
168 seedlings was measured. The germination index (GI) was calculated as follows: $GI (\%) = G Ls/Lc$,
169 where G is the percentage of germination obtained with respect to the control values, Ls is the
170 mean root length in the soil extracts, and Lc is the mean root length in the control.

171 **2.6 Statistical analysis**

172 Data were statistically treated using version 24.0 of the SPSS program for Windows. Analysis of
173 variance (ANOVA) and test of homogeneity of variance were carried out. In the case of
174 homogeneity ($p < 0.05$), a post hoc least significant difference (LSD) test was carried out. If
175 there was no homogeneity, Dunnett's T3 test was performed.

176 **3. Results and discussion**

177 **3.1 Soil characterization**

178 The initial soil properties are shown in Table S1 (Supplementary Material). Results revealed
179 typical characteristics of soils in arid areas, i.e. low organic matter and nitrogen content,
180 alkaline pH and a high carbonate content. The texture was sandy loam. The mean
181 concentrations of Cu, Ni, Pb, Zn, Cr, and Cd were below the current Regional Screening Levels
182 for industrial uses (BOJA, 2015). In contrast, the concentration of As was 30 times more than
183 the maximum permitted levels.

184 **3.2 Nanoparticle characterization**

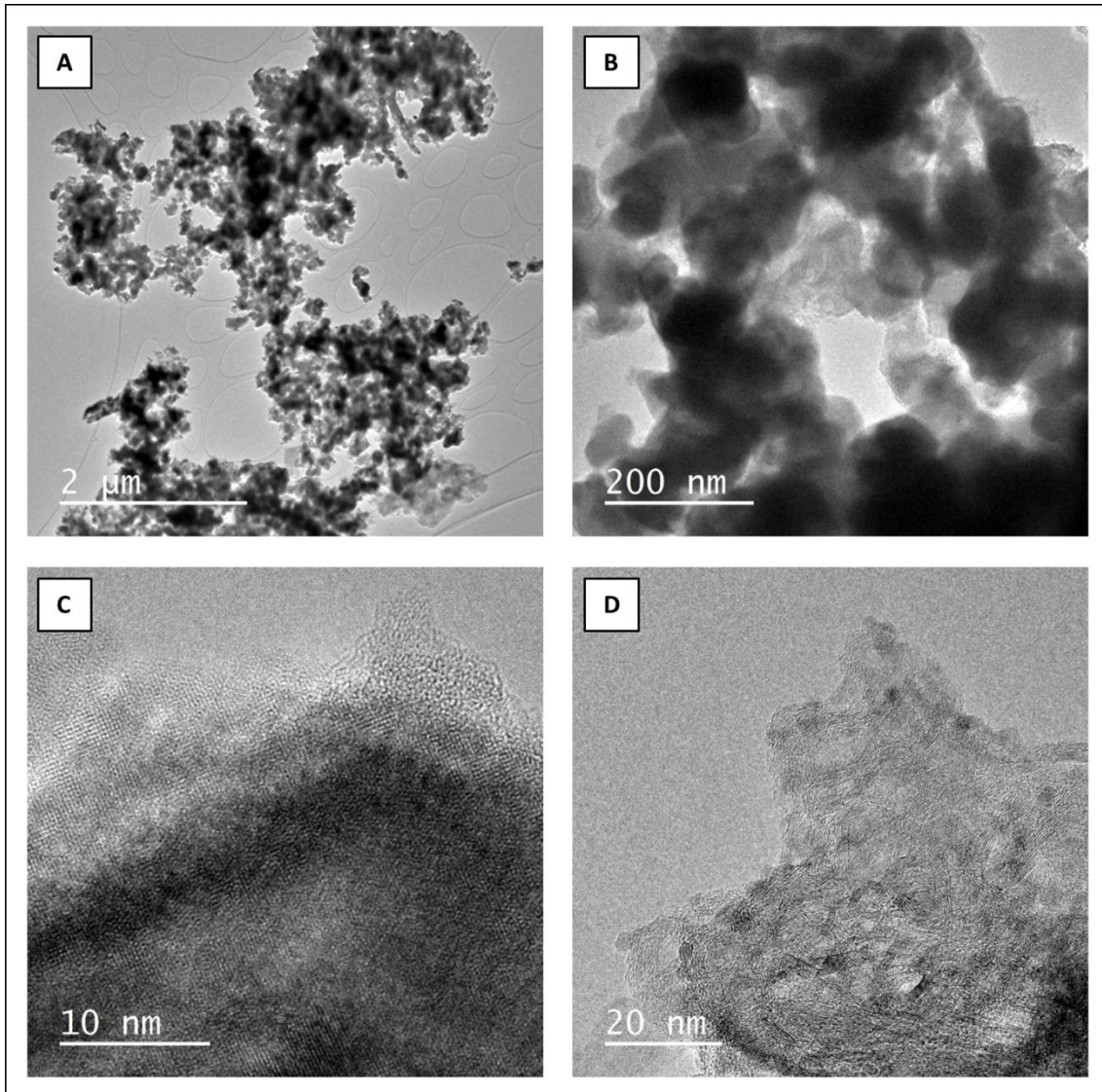
185 In brief, the NANOFER 25S slurry is an aqueous dispersion of stabilized nZVI. According to the
186 commercial specification, its Fe(0) content is 14-18%, and 2-6% of magnetite is also present,
187 the average size of the NPs is around 60 nm, the suspension is strongly alkaline (pH 11-12), and
188 the active surface area is 20 m²/g (additional details are available at www.nanoiron.cz).

189 In contrast, nGoethite are iron oxy-hydroxide (α -FeOOH) NPs dispersed in an aqueous solution.
190 Trace metal analysis revealed low concentrations (total concentration lower than 208 ppm) of
191 Ag, Al, Ba, Cd, Cr, Mg, Pb, Ti, W and Zn and a pH of 3.2 when in suspension, according to the
192 product's certificate of analysis.

193 Although nZVI (NANOFER 25s) have been previously described (Klimkova et al., 2011; Laumann
194 et al., 2013; Schmid et al., 2015), to extend knowledge about nGoethite and compare the two
195 types of NPs, additional analyses were carried out prior to the batch experiments. SEM images
196 of nZVI revealed a surface topography (Figure S1A, Supplementary Material) formed by
197 spheres of regular sizes. However, SEM images of nGoethite (Figure S1B, Supplementary
198 Material) showed a product with a blade shape. Regarding the chemical composition of nZVI
199 (Figure S1C, Supplementary Material) and nGoethite (Figure S1D, Supplementary Material), Fe

200 was found to be the predominant element in the former (more than 80% Fe), and a certain
201 degree of oxidation was observed (less than 20% O). In contrast, iron oxides were the main
202 components of nGoethite (only 60% Fe). Minor components were observed, such as Si and C,
203 which are related to the sample carrier composition.

204 TEM images of nZVI (Figure 1A and 1C) and nGoethite (Figure 1B and 1D) showed that the NPs
205 were not well distributed, probably due to the drying step carried out in the TEM sample
206 preparation. Therefore, DLS analysis was preferred in order to determine the nanoparticles
207 size. Regarding nZVI, the analysis revealed a diameter close to 60 nm which is consistent with
208 the commercial specification, whereas the average diameter of nGoethite was close to 2.7 nm.
209 Comparing size of nanoparticles distribution of both types, nGoethite are one order of
210 magnitude lower and the distribution is narrower than nZVI (Figure S2).



211

212 **Figure 1.** TEM pictures (A and C: nZVI; B and D: nGoethite) of iron nanoparticles.

213 The zeta potential of nZVI was -31.9 mV, a value that is attributed to the polyacrylic acid (PAA)
214 coating used to stabilize the particles, thereby preventing agglomeration caused by counter
215 attractive magnetic and van der Waals forces (Laumann et al., 2013). In contrast, the charge of
216 nGoethite was 86 mV, a positive value consistent with the low pH of the suspension (Giménez
217 et al., 2007).

218

219

220 **3.3 Batch experiment evaluation**

221 *3.3.1 Impact on As availability*

222 The two NP treatments significantly reduced As leachability at the four doses applied, as
223 shown by the TCLP test (Figure 2). Generally, high As immobilization percentages (80-99%)
224 were found in most of the doses, except for D1 of nZVI. However, generally speaking,
225 nGoethite showed greater As immobilization yields (82.5%, 99.3%, 99.7% and 99.8% at
226 increasing doses) than nZVI (41.6%, 89.5%, 96.2% and 97.6%).

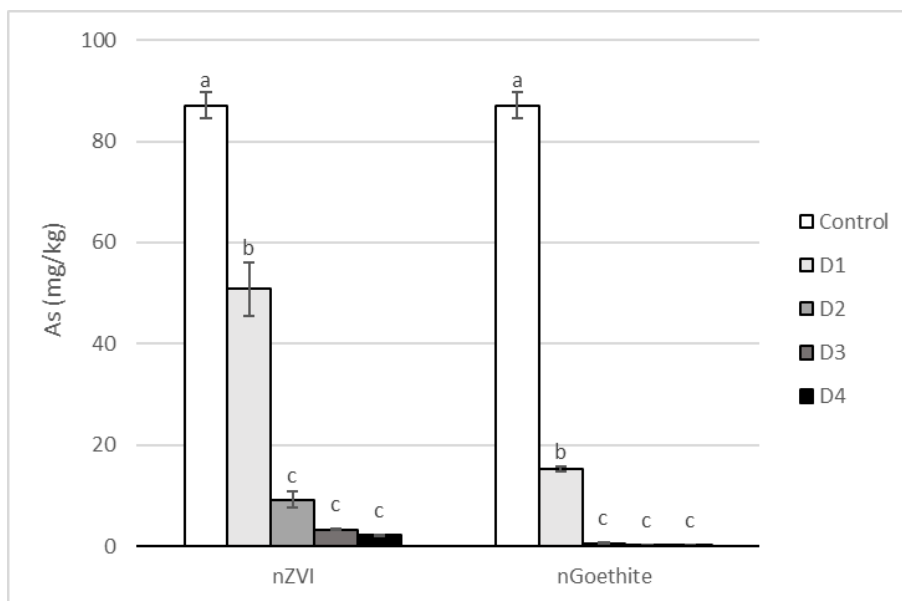


Figure 2. Mean concentration of arsenic (mg/kg) in TCLP extracts. For each type of nanoparticle, bars with the same letter do not differ significantly ($p < 0.05$).

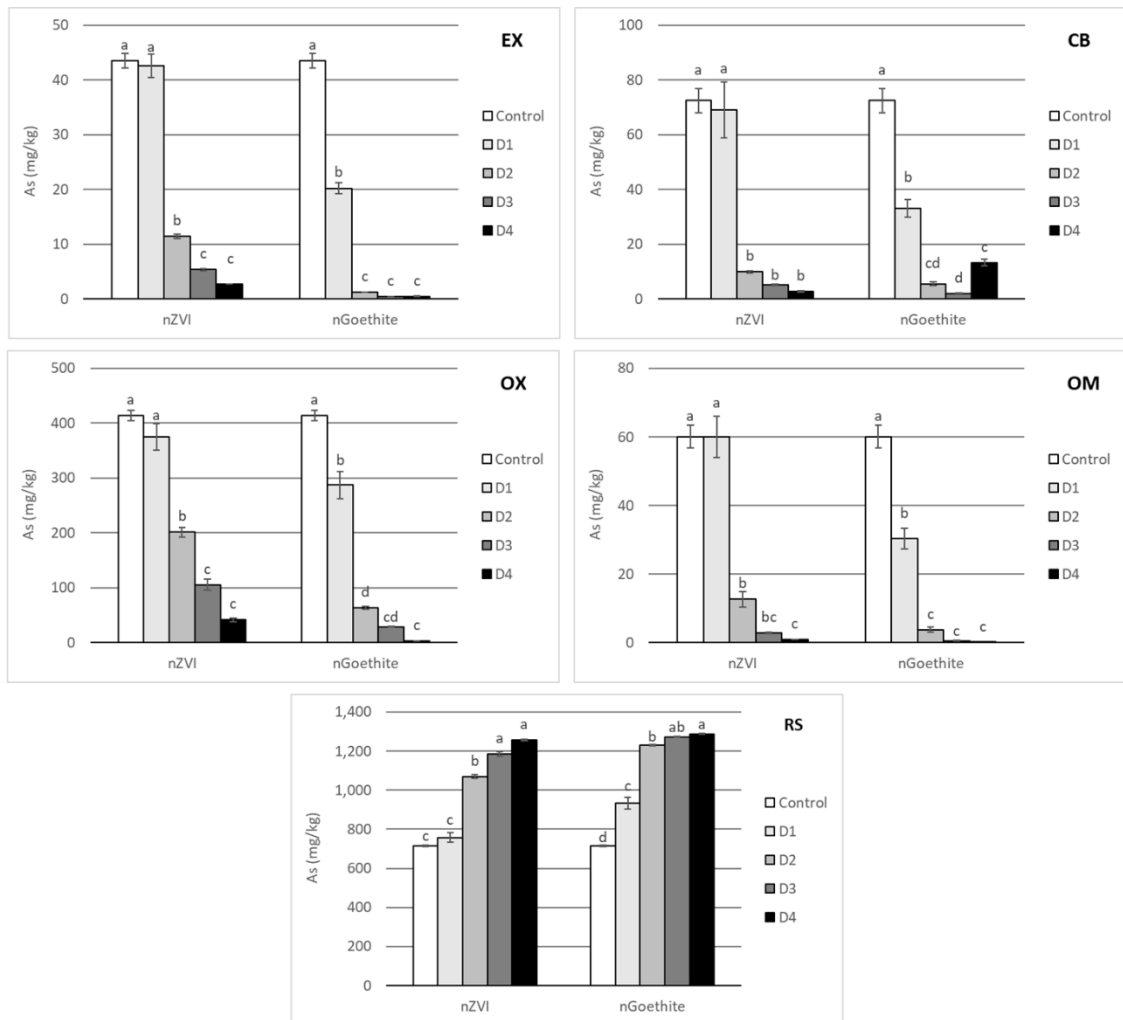
227

228 For all the Tessier fractions (Tessier et al., 1979), a common pattern of As distribution,
229 irrespective of the doses of NPs used, was observed (Figure 3), namely the RS fraction
230 increased, while the other fractions decreased. Only in the case of the lowest dose of nZVI was
231 a significant effect not detected. In this regard, previous studies using nZVI also reported a
232 significant increase in As associated with the RS fraction (Gil-Diaz et al., 2014, 2016, 2017a,
233 2017b).

234 Specifically, the concentration of As in the EX fraction was reduced after the treatment with
235 nZVI at doses D2, D3 and D4 (a reduction ranging from 74% to 94% was observed). In the case
236 of nGoethite, the As concentration in this fraction was reduced at all doses—53% at the lowest
237 dose and up to 99% at the highest. Thus, nGoethite at the lowest dose resulted significantly
238 more efficient than nZVI at reducing the As concentration in the most available fraction. In the
239 CB fraction, As concentration was only significantly reduced at D2, D3 and D4 using nZVI,
240 observing a reduction of between 86% and 96%. In contrast, nGoethite at the lowest dose
241 caused the concentration of As in the CB fraction to fall by 54%, while at higher doses, D2 and
242 D3, it reduced the concentration of this heavy metal in this fraction by up to 92% and 97%
243 respectively. However, at the highest dose, D4, the reduction fell to 82%. This decrease in
244 effectiveness might be due to the agglomeration of the NPs at such a high dosage or by some
245 other effect related to the pH, EC and Fe availability of the soil (Gil-Díaz et al. 2018; Singh and
246 Misra 2015). A similar decrease in As concentration to that observed in the most available
247 fractions was detected in the less mobile OX and OM fractions. Treatment with nZVI, except at
248 the lowest dose tested, led to a reduction in the OX and OM fractions, observing 50-90% and
249 79-99% decreases, respectively. nGoethite at all the doses tested led to significant reductions
250 in the OX and OM fractions, with decreases of 31-99% and 49-99.9%, respectively. Finally, the
251 concentration of As in the RS fraction, the non-available one, was significantly increased after
252 treatment with both types of NP at all doses, especially at the highest dose.

253 The reactivity and effectiveness of NPs for metal(oid) immobilization depend on the properties
254 of the NPs (e.g. size, coating, composition, surface charge) and soil conditions (Gil-Díaz et al.,
255 2017a). Regarding nZVI, this nanomaterial immobilizes As by adsorption onto iron oxides in the
256 shell surrounding the Fe(0) through inner-sphere surface complexation (Gil-Díaz et al., 2017a,
257 2014). Nevertheless, the surface chemistry of goethite differs to that of ZVI and varies with pH.
258 At low pH, the hydroxyl groups at the surface of goethite are doubly protonated ($\equiv\text{FeOH}_2^+$) and
259 the surface charge is thus positive (Giménez et al., 2007; O'Reilly et al., 2010), which is

260 consistent with the positive zeta potential value determined in the nGoethite characterization.
 261 At these acidic pH values, the electrostatic attraction between the negative oxoanions and the
 262 positive charge of the NPs favors adsorption (Siddiqui and Chaudhry, 2018). Therefore, the
 263 lower size of nGoethite NPs compared to nZVI, their corresponding higher specific surface, and
 264 adequate surface charge may explain the greater As immobilization achieved.



265
 266 **Figure 3.** Mean concentration of arsenic (mg/kg) in EX (exchangeable), CB (bound to
 267 carbonates), OX (bound to Fe-Mn oxides), OM (bound to organic matter) and RS (residual) soil
 268 fractions. For each type of nanoparticle, bars with the same letter do not differ significantly (p
 269 < 0.05).

270
 271 The results show that the application of Fe-based NPs, nZVI and nGoethite, to this industrial
 272 brownfield site significantly reduced the availability of As in the soil, as revealed by the TCLP

273 test and the Tessier method. The effectiveness of the As immobilization depends on the dose
 274 of NPs used, although doses of nZVI higher than 5%, as seen in previous studies (Gil-Díaz et al.,
 275 2017a, 2016a, 2014), and 1% of nGoethite did not show higher efficiency. The best
 276 stabilization results were obtained with nGoethite, even at the lowest dose tested (0.2%). The
 277 As immobilization capacity of this nanomaterial at such a low dose is a critical factor when
 278 considering field-scale remediation.

279 3.3.2 Impact on As speciation

280 The As speciation analysis in the original soil revealed that the predominant form of As (>96%)
 281 was arsenate (As^{5+}), whereas arsenite (As^{3+}) was below 4%. The reduction of As^{5+} to As^{3+}
 282 species by nZVI was reported by Ramos et al. 2009 in water samples under anaerobic
 283 conditions, although in previous studies with As-polluted soils (Gil-Díaz et al., 2017a, 2016a,
 284 2014), this reduction was not been detected. In our case, the addition of nZVI at the highest
 285 dose caused a minor but significant increase of 1.4% in As^{3+} (arsenite) proportion, a more
 286 mobile and phytotoxic form compared to As^{5+} (arsenate) (Table 1). Nevertheless, as shown
 287 above, As immobilization by adsorption onto iron oxides in the outer layer of the NPs reduced
 288 As availability, as measured by the TCLP test and Tessier extracts. Therefore, the main process
 289 involved in the immobilization of As was arsenate adsorption, although a reduction process
 290 was also present but to a minor extent, which can be explained by the core-shell structure of
 291 nZVI. On the other hand, the reduction mechanism was not observed when nGoethite was
 292 tested; i.e., no changes in speciation were observed (Table 1). This observation points to an
 293 additional advantage of nGoethite over nZVI under the experimental conditions tested.

294 **Table 1.** Arsenic speciation results for untreated samples and samples treated at the highest
 295 dose (D4). For each type of nanoparticle, data with the same letter do not differ significantly (p
 296 < 0.05). Note that mass recovery of the digestion method used is approximately 25% below of
 297 that obtained with aqua regia digestion.

Sample	As(III)	As(V)
Control	3.8±0.1a	96.2±0.1a
nZVI	5.2±0.6b	94.8±0.6b

nGoethite	3.5±0.1a	96.5±0.1a
-----------	----------	-----------

298

299 3.3.3 Impact on the pH and EC of soil

300 Given the different chemical nature of the two types of NPs applied and the differences of pH
 301 in the suspensions (the nZVI suspension was alkaline, while the nGoethite suspension was
 302 acidic), we examined their effects at a range of dosages on soil pH and EC.

303 The data are shown in Table S2. The application of nZVI did not affect pH or EC at any of the
 304 doses tested. However, nGoethite addition at the highest dose led to a significant decrease of
 305 pH, falling from 8.23 to 7.38. A lower pH enhances As immobilization. In relation to EC soil
 306 values, nGoethite induced a notable increase, ranging from 0.55 dS m⁻¹ at the lowest dose to
 307 5.38 dS m⁻¹ at the highest one. This increase should be taken into account from the point of
 308 view of soil functionality, as the highest dose (D4) will impair the biological activity of the soil
 309 and plant development. As immobilization was almost completed at moderate doses, thus it is
 310 suggested that the notable EC increase in doses D3 and especially in D4, is probably caused by
 311 an excess of nGoethite nanoparticles.

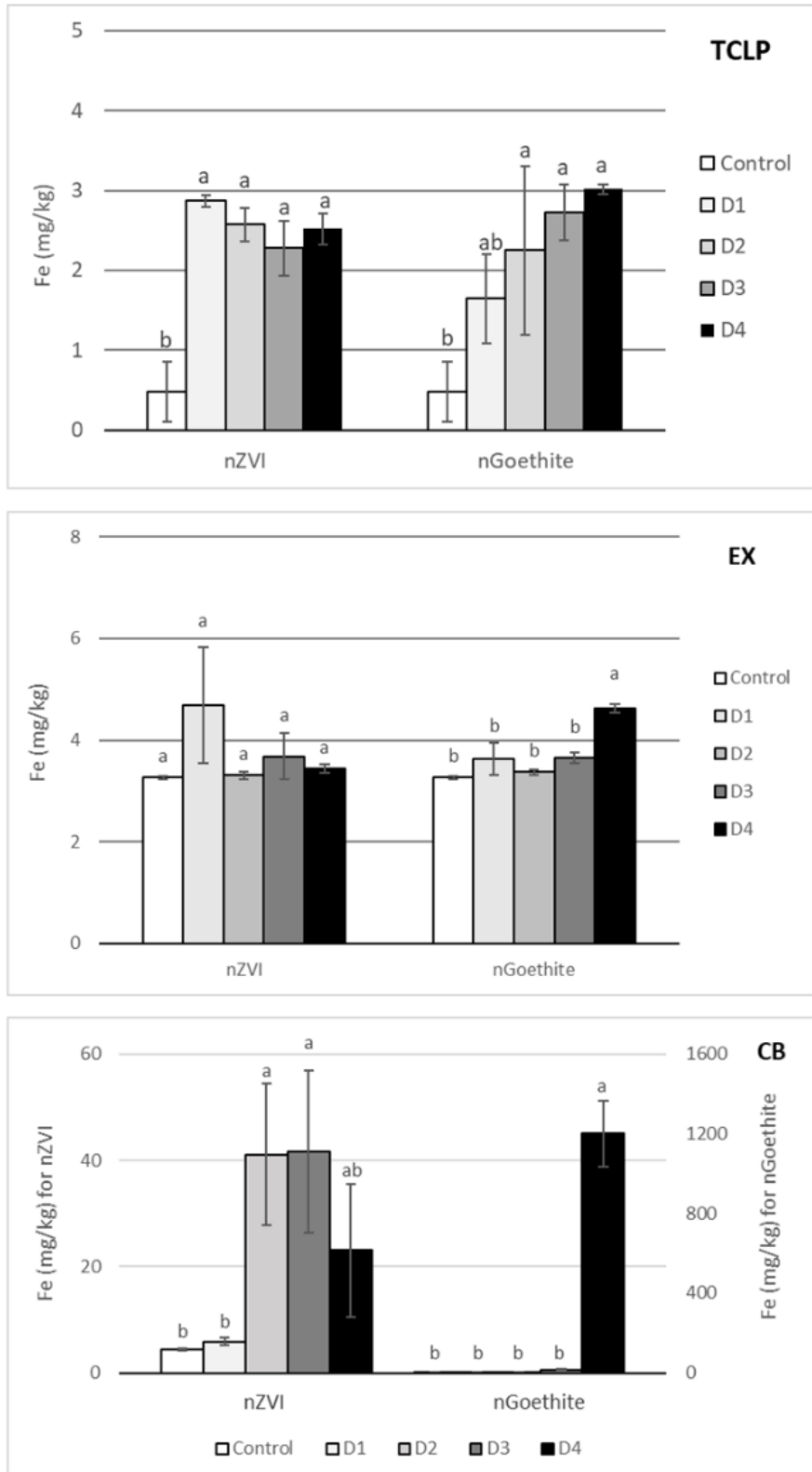
312 **Table 2.** Mean values and standard deviation of pH and electrical conductivity of soil samples
 313 treated with nZVI and nGoethite nanoparticles. For each type of nanoparticle, data with the
 314 same letter do not differ significantly ($p < 0.05$).

Treatment	Dose	pH	EC (dS/m)
Control	0%	8.23±0.04a	0.28±0.01a
nZVI	D1	8.58±0.10a	0.26±0.01a
	D2	8.48±0.09a	0.30±0.01a
	D3	8.63±0.11a	0.37±0.01b
	D4	9.05±0.20a	0.46±0.01c
nGoethite	D1	8.02±0.03ab	0.55±0.01b
	D2	8.00±0.09ab	1.56±0.02c
	D3	8.56±0.11a	2.43±0.07d
	D4	7.38±0.09b	5.38±0.03e

315

316 3.3.4 Impact on Fe availability

317 To determine the quantitative impact of the NP treatments on the availability of Fe in the soil,
 318 Fe concentration was measured. The Fe distribution in the TCLP extracts and in the most
 319 available Tessier fractions are showed in Figure 4.



320

321 **Figure 4.** Average concentration of iron (mg/kg) in TCLP extracts and in the EX (exchangeable)
322 and CB (bound to carbonates) soil fractions of the Tessier procedure. For each type of
323 nanoparticle, bars with the same letter do not differ significantly ($p < 0.05$).

324

325 The TCLP tests showed a slight increase in available Fe in all the treatments compared with
326 untreated soil. The increase was not dose-dependent.

327 Regarding the most available Tessier fractions, the addition of both types of NPs revealed a
328 different behavior.

329 The concentration of Fe in the EX fraction did not show significant variations for either type of
330 NP, with the exception of nGoethite treatment at the highest dose, which caused an increase
331 of 42%. This increase could be due to the extremely high dose; i.e., the Fe that has not reacted
332 with As and other soil components is in an available form.

333 In the CB fraction, Fe concentration increased between 430% and -856% in the nZVI treatment
334 at D2, D3 and D4. In the case of nGoethite treatment, no variation was observed in the CB
335 fraction, with the exception of the highest dose, in which a marked increase was detected,
336 probably attributable to the same reason as the increase in the EX fraction referred to above.

337 In summary, Fe is normally associated with the non-available fractions of Tessier extracts (Gil-
338 Díaz et al., 2016a, 2014). Therefore, in this case, it is particularly relevant that very small
339 differences and very low increases in Fe availability were observed for low doses of both nZVI
340 and nGoethite. However, medium and high doses of nZVI and the highest dose of nGoethite
341 led to a notable increase in the Fe bound to the CB fraction, and also to the EX fraction for
342 nGoethite.

343 *3.3.5 Soil phytotoxicity*

344 The results of the phytotoxicity assay are shown in Figure 5. According to Zucconi et al. (1985),
345 GI values below 50% indicate high phytotoxicity, between 50% and 80% moderate
346 phytotoxicity, and above 80% no phytotoxicity.

347 Initially, the untreated soil was highly phytotoxic to watercress since the GI of these plants was
348 <50%. The application of nZVI at all the doses tested significantly reduced phytotoxicity. These
349 results are consistent with those obtained from the sequential extraction procedure and TCLP
350 tests, which showed that treated soils showed a lower availability of As, the only contaminant
351 in the soil. The same effect was observed with the lowest dose of nGoethite, but not with the
352 higher ones. The latter observation can be explained by the dramatic increase in soil EC when
353 high amounts of nGoethite are added, as described above.

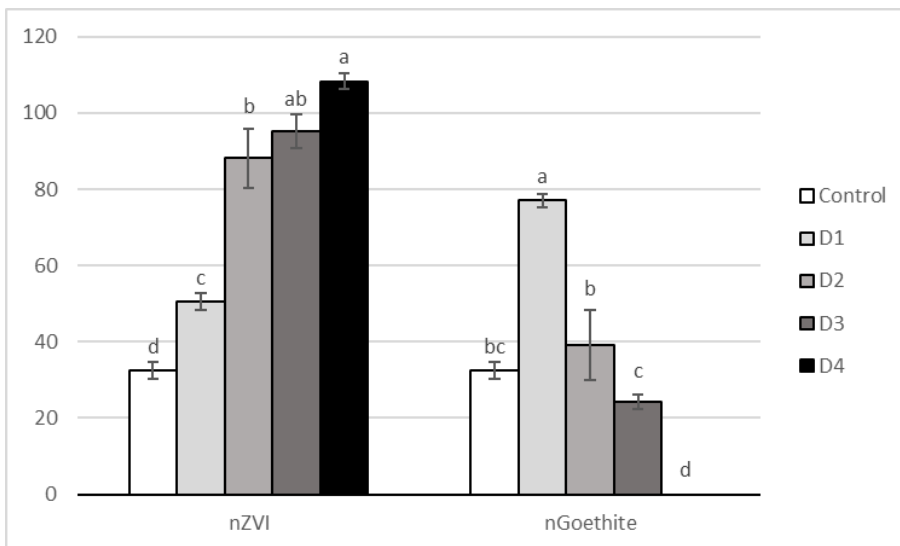


Figure 5. Mean germination index (%) of watercress for the soils treated with different doses of nanoparticles. For each type of nanoparticle, bars with the same letter do not differ significantly ($p < 0.05$).

354

355 4. Conclusions

356 The application of nZVI and nGoethite to soil samples from a brownfield polluted with As
357 caused a marked reduction in the availability of this heavy metalloid. The effectiveness of the
358 immobilization was significantly higher for nGoethite. However, the marked effect of high
359 doses of this nGoethite on the EC and phytotoxicity of soil may limit the use of this

360 nanomaterial for remediation purposes. The highest dose of nZVI (10% w/w) tested was
361 observed to cause a slight increase in arsenate reduction to arsenite (lower than 2%).

362 Our results demonstrate that both nZVI and nGoethite, at the lowest doses assayed (0.5% and
363 0.2 %, respectively) are efficient, although the former showed poorer As immobilization yields,
364 as revealed by measurements of As availability in the EX and CB fractions of the Tessier
365 method and in TCLP extracts. Moderate doses of nZVI outperformed nGoethite with respect to
366 As immobilization. However, some of the harmful effects of the highest doses nZVI, as
367 mentioned above, particularly its capacity to cause a slight increase in Fe availability, could
368 affect the appropriateness of this product.

369 On the basis of our findings, we conclude that, at the lowest dose assayed (0.2%), nGoethite is
370 a safe and promising technique for As immobilization. Regarding nZVI, a dose of 2% would
371 show a similar result for the remediation of the brownfield. Pilot or real-scale studies are now
372 required to validate these conclusions in a range of soil types.

373

374 **Acknowledgments**

375 This work was supported by the research projects REHABILITA CTM2016-78222-C2-1-R
376 AEI/FEDER, UE), FP-16-NANOREMED (IMIDRA, Comunidad de Madrid, Spain), and CTM2016-
377 75894-P (MINECO).

378 We would like also to thank the Environmental Assay Unit and the Electronic Microscope of
379 the Scientific and Technical Services of the University of Oviedo for technical support. Diego
380 Baragaño obtained a grant from the “Formación del Profesorado Universitario” program,
381 financed by the “Ministerio de Educación, Cultura y Deporte de España”.

382

383

384

385

386

387

388 **References**

389 **References**

390 Adriano, D.C., 2001. Trace Elements in Terrestrial Environments Biogeochemistry,
391 Bioavailability, and Risks of Metals, Volume I. <https://doi.org/10.1007/978-0-387-21510-5>

392 Aide, M., Beighley, D., Dunn, D., 2016. Arsenic In The Soil Environment : A Soil Chemistry
393 Review. *Int. J. Appl. Agric. Res.* 11, 1–28.

394 Alekseenko, V.A., Bech, J., Alekseenko, A. V., Shvydkaya, N. V., Roca, N., 2018. Environmental
395 impact of disposal of coal mining wastes on soils and plants in Rostov Oblast, Russia. *J.*
396 *Geochemical Explor.* 184, 261–270. <https://doi.org/10.1016/j.gexplo.2017.06.003>

397 Atkinson, R.J., Posner, A.M., Quirk, J.P., 1968. Crystal nucleation in Fe(III) solutions and
398 hydroxide gels. *J. Inorg. Nucl. Chem.* 30, 2371–2381. [https://doi.org/10.1016/0022-](https://doi.org/10.1016/0022-1902(68)80247-7)
399 [1902\(68\)80247-7](https://doi.org/10.1016/0022-1902(68)80247-7)

400 Baragaño, D., Rodríguez-Valdés, E., Peláez, A.I., Boente, C., Matanzas, N., García, N., Gallego,
401 J.L.R., 2018. Environmental Forensic Study and Remediation Feasibility in an Abandoned
402 Industrial Site. *Proceedings 2*, 1503. <https://doi.org/10.3390/proceedings2231503>

403 Boente, C., Matanzas, N., García-González, N., Rodríguez-Valdés, E., Gallego, J.R., 2017. Trace
404 elements of concern affecting urban agriculture in industrialized areas: A multivariate
405 approach. *Chemosphere* 183, 546–556.
406 <https://doi.org/10.1016/j.chemosphere.2017.05.129>

407 BOJA, Boletín Oficial de la Junta de Andalucía, 38, February 2015. Regulation that regulates the
408 regime applicable to contaminated soils.

409 https://www.juntadeandalucia.es/medioambiente/portal_web/web/temas_ambientales/suel
410 [o/suelos_contaminados/reglamento_suelos_contaminados.pdf](https://www.juntadeandalucia.es/medioambiente/portal_web/web/temas_ambientales/suel/o/suelos_contaminados/reglamento_suelos_contaminados.pdf) (Accessed February
411 2019).

412 Chen, Y.H., Li, F.A., 2010. Kinetic study on removal of copper(II) using goethite and hematite
413 nano-photocatalysts. *J. Colloid Interface Sci.* 347, 277–281.
414 <https://doi.org/10.1016/j.jcis.2010.03.050>

415 Davis, B.S., Birch, G.F., 2011. Spatial distribution of bulk atmospheric deposition of heavy
416 metals in metropolitan Sydney, Australia. *Water. Air. Soil Pollut.* 214, 147–162.
417 <https://doi.org/10.1007/s11270-010-0411-3>

418 Fajardo, C., Ortíz, L.T., Rodríguez-Membibre, M.L., Nande, M., Lobo, M.C., Martín, M., 2012.
419 Assessing the impact of zero-valent iron (ZVI) nanotechnology on soil microbial structure
420 and functionality: A molecular approach. *Chemosphere* 86, 802–808.
421 <https://doi.org/10.1016/j.chemosphere.2011.11.041>

422 Fajardo, C., Gil-Díaz, M., Costa, G., Alonso, J., Guerrero, A.M., Nande, M., Lobo, M.C., Martín,
423 M., 2015. Residual impact of aged nZVI on heavy metal-polluted soils. *Sci. Total Environ.*
424 535, 79–84. <https://doi.org/10.1016/j.scitotenv.2015.03.067>

425 Fendorf, S., Eick, M.J., Grossl, P., Sparks, D.L., 1997. Arsenate and chromate retention
426 mechanisms on goethite. 1. Surface structure. *Environ. Sci. Technol.* 31, 315–320.
427 <https://doi.org/10.1021/es950653t>

428 Forján, R., Asensio, V., Rodríguez-Vila, A., Covelo, E.F., 2016. Contribution of waste and biochar
429 amendment to the sorption of metals in a copper mine tailing. *Catena* 137, 120–125.
430 <https://doi.org/10.1016/j.catena.2015.09.010>

- 431 Fraga, C.G., Oteiza, P.I., Keen, C.L., 2005. Trace elements and human health. *Mol. Aspects Med.*
432 26, 233–234. <https://doi.org/10.1016/j.mam.2005.07.014>
- 433 Gallego, J.R., Ortiz, J.E., Sierra, C., Torres, T., Llamas, J.F., 2013. Multivariate study of trace
434 element distribution in the geological record of Roñanzas Peat Bog (Asturias, N. Spain).
435 Paleoenvironmental evolution and human activities over the last 8000calyr BP. *Sci. Total*
436 *Environ.* 454–455, 16–29. <https://doi.org/10.1016/j.scitotenv.2013.02.083>
- 437 Gallego, J.R., Rodríguez-Valdés, E., Esquinas, N., Fernández-Braña, A., Afif, E., 2016. Insights
438 into a 20-ha multi-contaminated brownfield megasite: An environmental forensics
439 approach. *Sci. Total Environ.* 563–564, 683–692.
440 <https://doi.org/10.1016/j.scitotenv.2015.09.153>
- 441 Gao, S., Goldberg, S., Herbel, M.J., Chalmers, A.T., Fujii, R., Tanji, K.K., 2006. Sorption processes
442 affecting arsenic solubility in oxidized surface sediments from Tulare Lake Bed, California.
443 *Chem. Geol.* 228, 33–43. <https://doi.org/10.1016/j.chemgeo.2005.11.017>
- 444 Gil-Díaz, M., Alonso, J., Rodríguez-Valdés, E., Pinilla, P., Lobo, M.C., 2014. Reducing the mobility
445 of arsenic in brownfield soil using stabilised zero-valent iron nanoparticles. *J. Environ. Sci.*
446 *Heal. - Part A Toxic/Hazardous Subst. Environ. Eng.* 49, 1361–1369.
447 <https://doi.org/10.1080/10934529.2014.928248>
- 448 Gil-Díaz, M., Diez-Pascual, S., González, A., Alonso, J., Rodríguez-Valdés, E., Gallego, J.R., Lobo,
449 M.C., 2016a. A nanoremediation strategy for the recovery of an As-polluted soil.
450 *Chemosphere* 149, 137–145. <https://doi.org/10.1016/j.chemosphere.2016.01.106>
- 451 Gil-Díaz, M., González, A., Alonso, J., Lobo, M.C., 2016b. Evaluation of the stability of a
452 nanoremediation strategy using barley plants. *J. Environ. Manage.* 165, 150–158.
453 <https://doi.org/10.1016/j.jenvman.2015.09.032>
- 454 Gil-Díaz, M., Alonso, J., Rodríguez-Valdés, E., Gallego, J.R., Lobo, M.C., 2017a. Comparing

455 different commercial zero valent iron nanoparticles to immobilize As and Hg in
456 brownfield soil. *Sci. Total Environ.* 584–585, 1324–1332.
457 <https://doi.org/10.1016/j.scitotenv.2017.02.011>

458 Gil-Díaz, M., Pinilla, P., Alonso, J., Lobo, M.C., 2017b. Viability of a nanoremediation process in
459 single or multi-metal(loid) contaminated soils. *J. Hazard. Mater.* 321, 812–819.
460 <https://doi.org/10.1016/j.jhazmat.2016.09.071>

461 Gil-Díaz, M., Lobo, M.C. 2018. Phytotoxicity of Nanoscale Zerovalent Iron (nZVI) in Remediation
462 Strategies in: *Phytotoxicity of Nanoparticles*. M. Faisal et al. (eds.), Springer International
463 Publishing AG, part of Springer Nature 2018. [https://doi.org/10.1007/978-3-319-76708-](https://doi.org/10.1007/978-3-319-76708-6_13)
464 [6_13](https://doi.org/10.1007/978-3-319-76708-6_13)

465 Gil-Díaz, M., Rodríguez-Valdés, E., Alonso, J., Baragaño, D., Gallego, J.R., Lobo, M.C. 2019.
466 Nanoremediation and long-term monitoring of brownfield soil highly polluted with As
467 and Hg. *Sci. Total Environ.* 675, 165-175. <https://doi.org/10.1016/j.scitotenv.2019.04.183>

468 Giménez, J., Martínez, M., de Pablo, J., Rovira, M., Duro, L., 2007. Arsenic sorption onto natural
469 hematite, magnetite, and goethite. *J. Hazard. Mater.* 141, 575–580.
470 <https://doi.org/10.1016/j.jhazmat.2006.07.020>

471 Gonçalves, J.R., 2016. The Soil and Groundwater Remediation with Zero Valent Iron
472 Nanoparticles, in: *Procedia Engineering*. pp. 1268–1275.
473 <https://doi.org/10.1016/j.proeng.2016.06.122>

474 González, A., García- Gonzalo, P., Gil-Díaz, M., Alonso, J., Lobo, M.C., 2019. Compost-assisted
475 phytoremediation of As-polluted soil. *Journal of Soils and Sediments*.
476 <https://doi.org/10.1007/s11368-019-02284-9>

477 Gopalakrishnan, A., Krishnan, R., Thangavel, S., Venugopal, G., Kim, S.J., 2015. Removal of
478 heavy metal ions from pharma-effluents using graphene-oxide nanosorbents and study of

479 their adsorption kinetics. *J. Ind. Eng. Chem.* 30, 14–19.
480 <https://doi.org/10.1016/j.jiec.2015.06.005>

481 Hartley, W., Edwards, R., Lepp, N.W., 2004. Arsenic and heavy metal mobility in iron oxide-
482 amended contaminated soils as evaluated by short- and long-term leaching tests.
483 *Environ. Pollut.* 131, 495–504. <https://doi.org/10.1016/j.envpol.2004.02.017>

484 Hartley, W., Lepp, N.W., 2008. Remediation of arsenic contaminated soils by iron-oxide
485 application, evaluated in terms of plant productivity, arsenic and phytotoxic metal
486 uptake. *Sci. Total Environ.* 390, 35–44. <https://doi.org/10.1016/j.scitotenv.2007.09.021>

487 Hasegawa, H., Rahman, I.M.M., Rahman, M.A., 2015. Environmental Remediation
488 Technologies for Metal-Contaminated Soils, *Environmental Remediation Technologies for*
489 *Metal-Contaminated Soils*. <https://doi.org/10.1007/978-4-431-55759-3>

490 Hopkins, J., Watts, P., Hosford, M., 2009. Contaminants in soil: updated collation of
491 toxicological data and intake values for humans Inorganic arsenic. Science report:
492 SC050021/TOX 1. Environment Agency.
493 [http://webarchive.nationalarchives.gov.uk/20140328084622/http://www.environment-](http://webarchive.nationalarchives.gov.uk/20140328084622/http://www.environment-agency.gov.uk/research/planning/64002.aspx)
494 [agency.gov.uk/research/planning/64002.aspx](http://www.environment-agency.gov.uk/research/planning/64002.aspx) (Accessed February 2019).

495 Hua, M., Zhang, S., Pan, B., Zhang, W., Lv, L., Zhang, Q., 2012. Heavy metal removal from
496 water/wastewater by nanosized metal oxides: A review. *J. Hazard. Mater.*
497 <https://doi.org/10.1016/j.jhazmat.2011.10.016>

498 Irem, S., Islam, E., Maathuis, F.J.M., Niazi, N.K., Li, T., 2019. Assessment of potential dietary
499 toxicity and arsenic accumulation in two contrasting rice genotypes: Effect of soil
500 amendments. *Chemosphere* 225, 104–114.
501 <https://doi.org/10.1016/j.chemosphere.2019.02.202>

502 Khalid, S., Shahid, M., Niazi, N.K., Murtaza, B., Bibi, I., Dumat, C., 2017. A comparison of

503 technologies for remediation of heavy metal contaminated soils. *J. Geochemical Explor.*
504 182, 247–268. <https://doi.org/10.1016/j.gexplo.2016.11.021>

505 Kim, K.R., Lee, B.T., Kim, K.W., 2012. Arsenic stabilization in mine tailings using nano-sized
506 magnetite and zero valent iron with the enhancement of mobility by surface coating. *J.*
507 *Geochemical Explor.* 113, 124–129. <https://doi.org/10.1016/j.gexplo.2011.07.002>

508 Klimkova, S., Cernik, M., Lacinova, L., Filip, J., Jancik, D., Zboril, R., 2011. Zero-valent iron
509 nanoparticles in treatment of acid mine water from in situ uranium leaching.
510 *Chemosphere* 82, 1178–1184. <https://doi.org/10.1016/j.chemosphere.2010.11.075>

511 Komárek, M., Vaněk, A., Ettler, V., 2013. Chemical stabilization of metals and arsenic in
512 contaminated soils using oxides - A review. *Environ. Pollut.*
513 <https://doi.org/10.1016/j.envpol.2012.07.045>

514 Kumpiene, J., Lagerkvist, A., Maurice, C., 2008. Stabilization of As, Cr, Cu, Pb and Zn in soil
515 using amendments - A review. *Waste Manag.* 28, 215–225.
516 <https://doi.org/10.1016/j.wasman.2006.12.012>

517 Lado, L.R., Hengl, T., Reuter, H.I., 2008. Heavy metals in European soils: A geostatistical analysis
518 of the FOREGS Geochemical database. *Geoderma* 148, 189–199.
519 <https://doi.org/10.1016/j.geoderma.2008.09.020>

520 Laumann, S., Micić, V., Lowry, G. V., Hofmann, T., 2013. Carbonate minerals in porous media
521 decrease mobility of polyacrylic acid modified zero-valent iron nanoparticles used for
522 groundwater remediation. *Environ. Pollut.* 179, 53–60.
523 <https://doi.org/10.1016/j.envpol.2013.04.004>

524 Li, Z., Greden, K., Alvarez, P.J.J., Gregory, K.B., Lowry, G. V., 2010. Adsorbed polymer and NOM
525 limits adhesion and toxicity of nano scale zerovalent iron to *E. coli*. *Environ. Sci. Technol.*
526 44, 3462–3467. <https://doi.org/10.1021/es9031198>

527 Cagigal, E., Ocejo, M., Gallego, J.R., Peláez, A.I., Rodríguez-Valdés, E., 2018. Environmental
528 Effects of the Application of Iron Nanoparticles for Site Remediation, in: Iron
529 Nanomaterials for Water and Soil Treatment. pp. 283–307.
530 <https://doi.org/10.1201/b22501-12>

531 Magiera, T., Zawadzki, J., Szuszkiewicz, M., Fabijańczyk, P., Steinnes, E., Fabian, K., Miszczak, E.,
532 2018. Impact of an iron mine and a nickel smelter at the Norwegian/Russian border close
533 to the Barents Sea on surface soil magnetic susceptibility and content of potentially toxic
534 elements. *Chemosphere* 195, 48–62.
535 <https://doi.org/10.1016/j.chemosphere.2017.12.060>

536 MAPA, 1994. *Métodos Oficiales de Análisis*. Secretaría General Técnica Ministerio de
537 Agricultura, Pesca y Alimentación, Madrid. vol. III, pp. 219–324.

538 Marker, B.R., 2018. Brownfield Sites. pp. 92–94. [https://doi.org/10.1007/978-3-319-73568-](https://doi.org/10.1007/978-3-319-73568-9_36)
539 [9_36](https://doi.org/10.1007/978-3-319-73568-9_36)

540 Mesa, V., Navazas, A., González-Gil, R., González, A., Weyens, N., Lauga, B., Gallego, J.R.,
541 Sánchez, J., Peláez, A.I., 2017. Use of Endophytic and Rhizosphere Bacteria To Improve
542 Phytoremediation of Arsenic-Contaminated Industrial Soils by Autochthonous *Betula*
543 *celtiberica*. *Appl. Environ. Microbiol.* 83. <https://doi.org/10.1128/aem.03411-16>

544 Mueller, N.C., Braun, J., Bruns, J., Černík, M., Rissing, P., Rickerby, D., Nowack, B., 2012.
545 Application of nanoscale zero valent iron (NZVI) for groundwater remediation in Europe.
546 *Environ. Sci. Pollut. Res.* 19, 550–558. <https://doi.org/10.1007/s11356-011-0576-3>

547 O’Carroll, D., Sleep, B., Krol, M., Boparai, H., Kocur, C., 2013. Nanoscale zero valent iron and
548 bimetallic particles for contaminated site remediation. *Adv. Water Resour.* 51, 104–122.
549 <https://doi.org/10.1016/j.advwatres.2012.02.005>

550 O’Reilly, S.E., Strawn, D.G., Sparks, D.L., 2010. Residence Time Effects on Arsenate

551 Adsorption/Desorption Mechanisms on Goethite. *Soil Sci. Soc. Am. J.* 65, 67.
552 <https://doi.org/10.2136/sssaj2001.65167x>

553 Pérez-Sanz, A., Vázquez, S., Lobo, M.C., Moreno-Jimenez, E., García, P., Carpena, R.O., 2013.
554 Soil Factor controlling arsenic availability for *Silene vulgaris*. *Commun. Soil Sci. Plan.*
555 44(1414), 2152-2167. <https://doi.org/10.1080/00103624.2013.799683>

556 Rahimi, S., Moattari, R.M., Rajabi, L., Derakhshan, A.A., Keyhani, M., 2015. Iron
557 oxide/hydroxide (α,γ -FeOOH) nanoparticles as high potential adsorbents for lead removal
558 from polluted aquatic media. *J. Ind. Eng. Chem.* 23, 33-43.
559 <https://doi.org/10.1016/j.jiec.2014.07.039>

560 Rahmani, A.R., Ghaffari, H.R., Samadi, M.T., 2010. Removal of Arsenic (III) from Contaminated
561 Water by Synthetic Nano Size Zerovalent Iron. *World Acad. Sci. Eng. Technol.* 4, 647-650.

562 Rao, L.N., 2014. Environmental impact of uncontrolled disposal of e-wastes. *Int. J. ChemTech*
563 *Res.* 6, 1343-1353.

564 Saccà, M.L., Fajardo, C., Costa, G., Lobo, C., Nande, M., Martin, M., 2014. Integrating classical
565 and molecular approaches to evaluate the impact of nanosized zero-valent iron (nZVI) on
566 soil organisms. *Chemosphere* 104, 184-189.
567 <https://doi.org/10.1016/j.chemosphere.2013.11.013>

568 Santucci, L., Carol, E., Tanjal, C., 2018. Industrial waste as a source of surface and groundwater
569 pollution for more than half a century in a sector of the Río de la Plata coastal plain
570 (Argentina). *Chemosphere* 206, 727-735.
571 <https://doi.org/10.1016/j.chemosphere.2018.05.084>

572 Schmid, D., Micić, V., Laumann, S., Hofmann, T., 2015. Measuring the reactivity of
573 commercially available zero-valent iron nanoparticles used for environmental
574 remediation with iopromide. *J. Contam. Hydrol.* 181, 36-45.

575 <https://doi.org/10.1016/j.jconhyd.2015.01.006>

576 Siddiqui, S.I., Chaudhry, S.A., 2018. A review on graphene oxide and its composites preparation
577 and their use for the removal of As³⁺ and As⁵⁺ from water under the effect of various
578 parameters: Application of isotherm, kinetic and thermodynamics. *Process Saf. Environ.*
579 *Prot.* <https://doi.org/10.1016/j.psep.2018.07.020>

580 Singh, R., Misra, V., 2015. Stabilization of zero-valent iron nanoparticles: role of polymers and
581 surfactants. *Handbook of nanoparticles*. Springer, [https://doi.org/10.1007/978-3-319-](https://doi.org/10.1007/978-3-319-13188-7_44-2)
582 [13188-7_44-2](https://doi.org/10.1007/978-3-319-13188-7_44-2)

583 Tessier, A., Campbell, P.G.C., Bisson, M., 1979. Sequential Extraction Procedure for the
584 Speciation of Particulate Trace Metals. *Anal. Chem.* 51, 844–851.
585 <https://doi.org/10.1021/ac50043a017>

586 Waychunas, G.A., Kim, C.S., Banfield, J.F., 2005. Nanoparticulate iron oxide minerals in soils
587 and sediments: Unique properties and contaminant scavenging mechanisms, in: *Journal*
588 *of Nanoparticle Research*. pp. 409–433. <https://doi.org/10.1007/s11051-005-6931-x>

589 Zhang, M.Y., Wang, Y., Zhao, D.Y., Pan, G., 2010. Immobilization of arsenic in soils by stabilized
590 nanoscale zero-valent iron, iron sulfide (FeS), and magnetite (Fe₃O₄) particles. *Chinese*
591 *Sci. Bull.* 55, 365–372. <https://doi.org/10.1007/s11434-009-0703-4>

592 Zucconi, F., Monaco, A., Forte, M., De Bertoldi, M., 1985. Phytotoxins during the stabilization
593 of organic matter, in: *Composting of Agricultural and Other Wastes*. pp. 73–86.

594